Pathway to $O(\sqrt{d})$ Complexity bound under Wasserstein metric of flow-based models

Anonymous authors
Paper under double-blind review

Abstract

We develop general analytical tools to estimate the error of flow-based generative models under the Wasserstein metric and to establish an upper bound on the sampling iteration complexity, measured in terms of $\mathcal{O}(\sqrt{\operatorname{Tr} C})$, where C is the covariance matrix of the prior distribution. When using the standard Gaussian as the prior, the posterior scales as $O(\sqrt{d})$, which is shown to be optimal when the target distribution is Gaussian. More precisely, we show that the error under W_2 metric can be explicitly controlled by two parts: the Lipschitzness of the push-forward maps of the backward flow, which scales independently of the dimension, and a local discretization error that scales with the square root of the trace of the covariance. The former one is related to the existence of Lipschitz changes of variables induced by the (heat) flow. The latter one consists of the regularity of the score function in both spatial and temporal directions. We validate the pathway in the flow-based generative model associated with the Föllmer process and 1-rectified flow under the Gaussian tail assumption and find their wide applications in the Bayesian inverse problems and general data distribution with bounded support. Furthermore, we design numerical experiments to validate the optimality of the analysis with respect to discretization and spatial dimension.

1 Introduction

The landscape of deep learning has been fundamentally reshaped by the emergence of powerful generative models, including Generative Adversarial Networks (GANs) (Goodfellow et al., 2014; Arjovsky et al., 2017), Variational Auto-encoders (VAEs) (Kingma & Welling, 2014; Kingma et al., 2019), and Normalizing Flows (Papamakarios et al., 2021; Wang et al., 2023; Wan & Wei, 2022). These models have demonstrated remarkable success across diverse modalities such as images, audio, and text, by learning complex data distributions and generating high-quality samples (Achiam et al., 2023; Song et al., 2021).

Diffusion models (DM) are the state-of-the-art generative models, which can be analyzed via the SDE framework (Song et al., 2021). With the same forward and backward marginal as DM, flow-based models (Chen et al., 2023b;c) are generative models with deterministic flow given initial distribution, offering a principled framework for generative modeling and statistical inference (Cheng et al., 2024).

From a theoretical perspective, convergence guarantees of generative models are typically established under distributional discrepancies such as KL divergence, total variation, or Wasserstein distance. Early works primarily focus on KL-based analysis (Chen et al., 2023a; Benton et al., 2024; Conforti et al., 2025a; Li et al., 2024), which enables tractable error control via tools such as Girsanov's theorem. However, in many practical applications involving structured data (e.g., images or biological data), the target distribution often lies on a low-dimensional or compact sub-manifold of the ambient space (Tenenbaum et al., 2000; Bengio et al., 2017). In such settings, KL divergence becomes ill-defined or fails to capture meaningful geometric discrepancies.

This motivates the study of generative models under the Wasserstein metric, particularly the W_2 distance, which remains well-defined under finite second moments and is better suited for structured distributions.

However, analyzing convergence under W_2 is significantly more challenging. Unlike KL-based methods, Wasserstein analysis suffers from the accumulation of local discretization errors in Lyapunov-type estimates due to the lack of contractivity in reverse-time dynamics. Existing works mitigate this issue by imposing strong structural assumptions such as log-concavity (Gao & Zhu, 2025; Bruno & Sabanis, 2025). In particular, Proposition 6 in Gao et al. (2025) establishes that for the standard Gaussian as target distribution, $\mathcal{O}(\sqrt{d})$ complexity bound is optimal. In efforts to obtain complexity bounds under assumptions more general than log-concavity, recent works Bruno & Sabanis (2025) derived an $\mathcal{O}(d)$ bound using the weakly log-concave assumption Conforti (2024); Conforti et al. (2025b), and Gentiloni-Silveri & Ocello (2025) obtained an $\mathcal{O}(d^2)$ bound under the similar assumption. Despite Chen et al. (2023b) claiming the ODE type flow is provably fast by showing an $\mathcal{O}(\sqrt{d})$ bound under a predictor-corrector scheme, the analytical pathway to $\mathcal{O}(\sqrt{d})$ complexity upper bound for practical ODE flow based models in the non-log-concave setting remains unclear.

In light of this, **the main contribution of this paper** is to provide analytical tools that study the accumulation error along the sampling flow under the Wasserstein metric and hence ensure the optimal iteration complexity bound $O(\sqrt{d})$. Our analysis reveals that the W_2 distance between the generated and target distributions is governed by the Lipschitz regularity of the push-forward maps induced by the sampling flow. In addition, we identify the temporal regularity of the velocity field, namely $\partial_t V$, as a key factor controlling the local truncation error and thus the overall complexity. To establish these results, we introduce a general Gaussian tail assumption that ensures well-posedness and dimension-free Lipschitz bounds for the Föllmer flow. Under this condition, we obtain explicit control of both spatial and temporal regularity, leading to an optimal iteration complexity of $\mathcal{O}(\sqrt{d})$ without requiring log-concavity. Our framework also extends naturally to deterministic flows, infinite-dimensional settings, and Bayesian inverse problems. The numerical experiments presented in the later section further support these theoretical findings.

Table 1: Complexity bounds for DM/flow-based models in d dimensions: previous results vs. ours. The complexity bound is measured by number of steps needed to ensure error under Wasserstein metric is less than ϵ_0.

Target P_0	**Complexity**	**Result**
P_0 log-concave*	$\mathcal{O}\left(\frac{\sqrt{d}}{\epsilon_0}(\log\frac{d}{\epsilon_0})^2\right)$	Gao & Zhu (2025) Tab. 1
G-tail Ass.*	$\mathcal{O}\left(\frac{\sqrt{d}}{\epsilon_0}\log\frac{d}{\epsilon_0^2}\right)$	Wang & Wang (2024) Cor. 3.5
one-side Lip+weakly log-concave*	$\mathcal{O}\left(\frac{d^2}{\epsilon_0^2}\right)$	Gentiloni-Silveri & Ocello (2025) Thm. 3.5
weakly log-concave*	$\mathcal{O}\left(\frac{d}{\epsilon_0^2}\right)$	Bruno & Sabanis (2025) Thm. 3.12
G-tail Ass. 8	$\mathcal{O}\left(\frac{\sqrt{d}}{\epsilon_0}\right)$	Our Thm. 16

* denotes works on diffusion models.

1.1 Related Work

Lipschitz transport and flow regularity. The study of Lipschitz transport maps originates from Caffarelli's contraction theorem (Caffarelli, 2000) and has been extended to various settings including compact support (Colombo et al., 2017), diffusion processes (Kim & Milman, 2012), and Föllmer flows (Dai et al., 2023; Mikulincer & Shenfeld, 2023). Recent works further improve Lipschitz bounds under weaker assumptions (Neeman, 2022; Fathi et al., 2024; Brigati & Pedrotti, 2024). For clarity, we summarize the assumptions on target distributions and their Lipschitz constants in Table 2 of Appendix A. Despite these results shed light on potential minimal assumption for the convergence guarantee of flow-based models, in later context, we will demonstrate that estimation of the time derivative of velocity field $\partial_t V$ is also crucial on the pathway of optimal complexity bounds.

Continuous generative flows. Building on score-based (Song et al., 2021) and diffusion models (Gao & Zhu, 2025), recent works improve sampling efficiency via distillation (Salimans & Ho, 2022) and continuous flow formulations. Flow matching (FM) (Lipman et al., 2023) extends continuous normalizing flows (CNFs) (Chen et al., 2018) by learning neural ODE velocity fields that match prescribed probability paths, unifying diffu-

sion and non-diffusion models. Rectified flow (Liu et al., 2023; Rout et al., 2024) further constructs nearly straight transport trajectories, enabling efficient one-step generation. Stochastic interpolants (Albergo et al., 2023; Albergo & Vanden-Eijnden, 2023) provide a unified framework bridging flow-based and diffusion models, recovering the Schrödinger bridge when optimized (Léonard, 2013). More recently, Flow Map Matching (FMM) (Boffi et al., 2025) accelerates sampling via two-time flow maps, while Geng et al. (2025) connects one-step generative modeling with multiscale physical simulations, achieving strong performance on ImageNet 256×256.

Convergence bounds. Recent studies establish convergence guarantees under KL, W_2, or TV distances. For example, Albergo & Vanden-Eijnden (2023) bounds the W_2 error under Lipschitz assumptions, while Gao et al. (2024) and Cheng et al. (2024) provide KL-based complexity results. While these works deriving the Wasserstein error bounds with the assumption of Lipschitz-ness, the assumption in Theorem 6 of this work is more realistic and consistent with the estimates for the continuous flow.

1.2 Contributions

- We point out that the W_2-distance between the generative and target distributions is controlled by the Lipschitzness of the push-forward maps introduced by sampling flow. By providing concrete bounds on the Lipschitz coefficient, we obtain an explicit estimate of the accumulation error.
- While prior works often rely on smoothness or strict log-concavity, we adopt a general condition in applications-the Gaussian tail Assumption 8 to provide the well-posedness and Lipschitz regularity of Föllmer flow, with explicit, dimension-free Lipschitz bounds (Corollary 12 and Corollary 15).
- By leveraging the Gaussian tail Assumption 8 to obtain accurate upper bounds on the time derivative of velocity field $|\partial_t V|$ (Theorem 9), our framework avoids the need for end-point constraints or early stopping (Lyu et al., 2022), enabling training and sampling throughout the entire interval $t \in [0, 1]$. This framework naturally extends the $\mathcal{O}\left(\sqrt{d}\right)$ complexity results of the SDE flow to the deterministic flow, achieving even better complexity than previous approaches (Wang & Wang, 2024).
- Using an Föllmer flow sampler with an explicit score function, we study the Euler discretization error and observe first-order convergence in time. The experiments further confirm the predicted dimension scaling $N(d) \sim d^{0.5}$, with a fitted slope of approximately 0.472 in log–log regression.

2 Flow-based Model

We begin by introducing a unified formulation of flow-based generative models. This general framework allows the convergence analysis in Section 3 to apply seamlessly to both the Föllmer flow and more general sampling dynamics. Consider a continuous flow governed by a velocity field V via the ODE[1]

$$\frac{\mathrm{d}\overleftarrow{X}_t}{dt} = V\big(t, \overleftarrow{X}_t\big), \quad \overleftarrow{X}_0 = x, \quad t \in [0, 1]. \tag{1}$$

With the N steps discretization in time, $0 = t_0 < t_1 < \cdots < t_N = 1$, the ODE equation 1 in each sub-interval $[t_n, t_{n+1}]$, can be interpreted as a local transport map,

$$T_n(\overleftarrow{X}_{t_n}) = \overleftarrow{X}_{t_{n+1}}. \tag{2}$$

The overall flow-based model $\overleftarrow{X}_1(x)$ is then obtained by the composition of transport maps

$$\overleftarrow{X}_1(x) = (T_{N-1} \circ T_{N-2} \circ \cdots \circ T_0)(x).$$

An approximation of $\overleftarrow{X}_1(x)$ can be interpreted as approximation of $\{T_n\}_{n=0}^{N-1}$ by $\{\widetilde{T_n}\}_{n=0}^{N-1}$. To quantify the error of the approximation, we denote the marginal distribution of the actual state $\overleftarrow{X}_{t_{n+1}}$ by $\overleftarrow{P}_{t_{n+1}}$, and

[1]We used the left arrow $\overleftarrow{\cdot}$ to represent its connections to the backward process in the score-based model.

$\overleftarrow{Q}_{t_{n+1}}$ of the approximated state. Correspondingly we have,

$$\overleftarrow{P}_{t_{n+1}} = (T_n)_{\#}(\overleftarrow{P}_{t_n}), \quad \overleftarrow{Q}_{t_{n+1}} = (\widetilde{T}_n)_{\#}(\overleftarrow{Q}_{t_n}). \tag{3}$$

Föllmer flow For any $\varepsilon \in (0,1)$, we consider a diffusion process $(\overrightarrow{X}_t)_{t\in[0,1-\varepsilon]}$ that gradually transforms the target distribution ν into a Gaussian $\mathcal{N}(0,C)$ over time by the following Itô SDE

$$d\overrightarrow{X}_t = -\frac{1}{1-t}\overrightarrow{X}_t dt + \sqrt{\frac{2C}{1-t}}dW_t, \quad \overrightarrow{X}_0 \sim \nu, \quad t \in [0, 1-\varepsilon], \tag{4}$$

where W_t is a standard Brownian motion, C is a symmetric, positive-definite covariance matrix. The transition probability distribution from $\overrightarrow{X}_0$ to $\overrightarrow{X}_t$ is given by

$$\overrightarrow{X}_t | \overrightarrow{X}_0 = x_0 \sim \mathcal{N}\big((1-t)x_0, t(2-t)C\big). \tag{5}$$

The marginal distribution flow $(\bar{p}_t)_{t\in[0,1-\varepsilon]}$ of the forward diffusion process satisfies the Fokker-Planck-Kolmogorov (FPK) equation in an Eulerian framework

$$\partial_t \bar{p}_t = \nabla \cdot \left(\bar{p}_t \cdot \frac{1}{1-t}[x + C\nabla \log \bar{p}_t(x)] \right) \quad \text{on } [0, 1-\varepsilon] \times \mathbb{R}^d, \quad \bar{p}_0 = \nu. \tag{6}$$

Then Föllmer flow is formally defined as the backward process of such a forward diffusion equation 4, while preserving the same marginal distributions in equation 6.

Definition 1 (Föllmer flow in formal sense)**.** *A Föllmer flow* $(\overleftarrow{X}_t)_{t\in[0,1]}$ *solves the IVP*

$$\begin{cases} \frac{\mathrm{d}\overleftarrow{X}_t}{\mathrm{d}t} = V(t, \overleftarrow{X}_t), \quad \overleftarrow{X}_0 \sim \gamma_C, \quad t \in [0,1], \\ V(t,x) := \frac{1}{t}\left[x + S(t,x)\right], \quad \forall t \in (0,1]; \qquad V(0,x) := \sqrt{C}\mathbb{E}_\nu[X], \end{cases} \tag{7}$$

$S(t,x) := C\nabla \log p_t(x)$ is the score function with probability density $p_t = \bar{p}_{1-t}$ in forward FKP equation equation 6. We call $V(t,x)$ a Föllmer velocity field.

Following equation 3, we define $\overrightarrow{P}_{t_n}$ as the marginal distribution of $\overrightarrow{X}_{t_n}$ in the forward diffusion process. Given the initial distribution $\overrightarrow{P}_0 = P_{\text{data}}$, then for all $t \in [0,1]$, $\overleftarrow{P}_{t_n} = \overrightarrow{P}_{1-t_n}$.

In practice, the velocity field $V(1-t,x) = \frac{1}{1-t}\left[x + C\nabla \log \bar{p}_t(x)\right]$ is not available since no closed form expression of $\bar{p}_t$ is known. To this end, one approximates V by a neural network $\widetilde{V}$. The network is trained by minimizing an $\mathbb{L}_2$ estimation loss,

$$\mathbb{E}_{\bar{p}_t(x)} \left\| \widetilde{V}(1-t,x) - \frac{1}{1-t}\left[x + C\nabla \log \bar{p}_t(x)\right] \right\|^2. \tag{8}$$

For simplicity, we introduce the notation $X_t := (1-t)X_0 + \sqrt{t(2-t)C}\,\mathcal{N}$, which shares the same marginal distribution as $\overrightarrow{X}_t$ in equation 5. Then the velocity field $V(1-t,x)$ can be expressed as a conditional expectation (Yubin et al., 2025),

$$V(1-t,X) := \frac{1}{1-t}\big[X + S(1-t,X)\big] = \mathbb{E}_{X_0|X_t}\left[\frac{1}{1-t}X_t - \frac{X_t - (1-t)X_0}{(1-t)t(2-t)} \,\middle|\, X_t = X \right].$$

With an appropriate weight of the t-variable, the loss in equation 8 becomes an approximation of this conditional expectation via mean-squared prediction error,

$$\mathbb{E}_{X_0,\, N\sim\mathcal{N}(0,I_d),\, t}\left[\lambda(t) \left\| \widetilde{V}\left(1-t, X_t\right) - \frac{1}{1-t}X_t + \frac{\sqrt{C}\mathcal{N}}{(1-t)\sqrt{t(2-t)}} \right\|^2 \right]. \tag{9}$$

After training, with $\widetilde{V}(1-t,x)$, one can generate samples of the target distribution via an Euler-type discretization of the continuous-time process, starting from the Gaussian initialization γ_C,

$$\frac{\mathrm{d}\overleftarrow{Y}_t}{dt} = \widetilde{V}(t_n, \overleftarrow{Y}_{t_n}), \quad \overleftarrow{Y}_{t_0} \sim \gamma_C, \quad t \in [t_n, t_{n+1}], \quad n = 0, 1 \ldots, N-1. \tag{10}$$

Note that equation 10 defines the transport map $\widetilde{T}_n$ for the learned Föllmer flow, governed by the approximate velocity field $\widetilde{V}(t_n, \overleftarrow{Y}_{t_n})$ over the sub-interval $[t_n, t_{n+1}] \subset [0,1]$. Distribution of generation $\overleftarrow{Q}_t$ is then defined by equation 3.

Well-posedness of Föllmer flow Under appropriate assumptions on the target distribution ν, one can show the Föllmer flow being the time-reversal of the forward diffusion process equation 4. For instance, under third moment (Assumption 7), semi-log-convexity and the structural assumptions on ν, Dai et al. (2023) studied the Föllmer flow in the case $C = I_d$, where the score function is given by

$$S(t,x) := \nabla \log \int_{\mathbb{R}^d} (2\pi(1-t^2))^{-\frac{d}{2}} \exp\left(-\frac{|x-ty|^2}{2(1-t^2)}\right) \nu(dy).$$

It can be shown that the velocity field V is Lipschitz continuous in x with a well-defined initial condition $V(0,x)$. By the Cauchy-Lipschitz theory (Ambrosio & Crippa, 2014), one can define a Lagrangian flow $(X_t^*)_{t\in[0,1]}$ governed by the well-posed ODE system,

$$dX_t^* = -V(1-t, X_t^*)dt, \quad X_0^* \sim \nu, \quad t \in [0,1],$$

sharing the same marginal distribution with equation 4.

In this work, we study the Föllmer flow with correlated Gaussian initial based on the Gaussian tail Assumption 8, and retain the spatially anisotropic noise assumption ($C \neq I_d$) to allow our theory to generalize to infinite-dimensional settings requiring compactification (Lim et al., 2025); We refer the reader to Theorem 9 for the regularity of the velocity field and Lemma 11 for the proof of well-posedness.

General Notations Let γ_C denote the density of $\mathcal{N}(0,C)$. For an $n \times n$ matrix A, the operator norm $\|\cdot\|$ is defined as

$$\|A\| = \sup_{v\neq 0} \frac{|Av|}{|v|} = \text{largest eigenvalue of } \sqrt{A^T A}.$$

For symmetric positive-definite A, define the weighted ℓ_2 norm

$$|x|_A^2 := (A^{-1/2}x, A^{-1/2}x),$$

which reduces to the standard ℓ_2 norm $|\cdot|$ when $A = I$. For a vector (matrix)-valued function $f(x)$,

$$|f|_\infty = \sup_x |f(x)|, \quad (\|f\|_\infty = \sup_x \|f(x)\|).$$

3 General Theory to the optimal complexity bound

In this section, we present the main results. Our analysis begins with a general flow-based framework (not necessarily restricted to the Föllmer flow), through which we develop Wasserstein-based analytical tools that yield an optimal iteration complexity bound of $\sqrt{d}$. We then validate the assumptions and present the complexity results for the Föllmer flow and 1-rectified flow under the Gaussian tail assumption.

3.1 Lipschitz changes of variables imply Wasserstein bound of flow-based models

For the sake of compactness, we impose the following assumption on the second-order moment.

Assumption 2 (Second moment)**.** *The data distribution has a bounded second moment,* $M_2 := \mathbb{E}_{p_0}|x|^2 < \infty$*. We further denote,*

$$M_0 = \max\{\mathrm{Tr}(C), M_2\},$$

relates to the maximum second-order moment, where C *is a symmetric, positive-definite covariance matrix.*

We consider a general covariance matrix C to cover both the standard Gaussian case $C = I_d$ and the anisotropic noise case $C \neq I_d$. For the former one, by $\mathrm{Tr}(C) = d$ and thus $M_0 = \mathcal{O}(d)$, we aim to obtain the optimal dependence. At the same time, we retain $C \neq I_d$ in the derivation to extend our theory to infinite-dimensional settings (Lim et al., 2025), with the general case further discussed in Appendix B.10 for Bayesian inverse problems.

Next, we make three assumptions, each holding with some dimension-free constants. We regard these assumptions as generally valid, and under them, our convergence result Theorem 6 can be established.

Assumption 3 (Lipschitzness of T)**.** $\forall n = 0, \ldots, N-1$, $\mathrm{Lip}(T_n) < \infty$*, and* $\prod_{j=0}^{n} \mathrm{Lip}(T_j) < \infty$*.*

We will justify the attainability of the Assumption 3 in Corollary 12 by invoking the Lipschitz property of the velocity field established in Theorem 9. Similar to Assumption 3 which imposes Lipschitz continuity of T, we also assume the Lipschitz continuity of $\widetilde{T}$ as stated below.

Assumption 4 (Lipschitzness of $\widetilde{T}$)**.** $\forall n = 0, \ldots, N-1$, $\mathrm{Lip}(\widetilde{T}_n) < \infty$*, and* $\prod_{j=0}^{n} \mathrm{Lip}(\widetilde{T}_j) < \infty$*.*

We will verify Assumption 4 in Corollary 15 by leveraging the Lipschitz property of the learned velocity field stipulated in Assumption 14. The final assumption concerns the local discretization error between T and $\widetilde{T}$ at each time step h, as described below.

Assumption 5 (Accuracy of approximation)**.** *There exists constants* $\overline{K}$*,* $\overline{K_1}$*,* $\overline{K_2}$*,* ϵ*, such that*

$$\sqrt{\mathbb{E}_{x \sim \overleftarrow{P}_{t_n}} |\widetilde{T}_n(x) - T_n(x)|^2} \leq h \left(\left(\overline{K}\sqrt{M_0} + \frac{\overline{K_1}}{\sqrt{1-t_n^2}} + \overline{K_2} \right) h + \epsilon \right),$$

with time step size $h = t_{n+1} - t_n$*.*

This scaling follows since

$$\widetilde{T}_n(x) - T_n(x) = h\big(V(x) - \widetilde{V}(x)\big) + \mathcal{O}(h^2),$$

as verified in the Föllmer case Theorem 16. The term $\mathcal{O}(h)$ reflects the ϵ-accuracy of the learned velocity $\widetilde{V}(x)$ (Assumption 13), while the term $\mathcal{O}(h^2)$ stems from the Taylor expansion of $T_n(x)$ over $[t_n, t_{n+1}]$ and depends on its regularity, possibly also on ambient dimension d and time t.

Next, we outline the core proof strategy of this work. The key step is to demonstrate the Lipschitz continuity of both the original and discretized flows, which is critical for guaranteeing the convergence of flow-based generative models.

Theorem 6. *Assume that the target distribution satisfies Assumption 2 and follows Lipschitzness Assumption 3, 4, and approximation error Assumption 5. With constant step size* h*, the Wasserstein-2 distance between the target distribution* $\overrightarrow{P}_0 = \overleftarrow{P}_1$ *and the generation* $\overleftarrow{Q}_1$ *is bounded as,*

$$\begin{aligned} \mathcal{W}_2(\overleftarrow{P}_1, \overleftarrow{Q}_1) \leq & \left(\prod_{j=0}^{N-1} \mathrm{Lip}(\widetilde{T}_j) \right) \mathcal{W}_2(\overleftarrow{P}_0, \overleftarrow{Q}_0) \\ & + h \sum_{k=0}^{N-2} \prod_{j=k}^{N-2} \mathrm{Lip}(\widetilde{T}_j) \left(\left(\overline{K}\sqrt{M_0} + \frac{\overline{K_1}}{\sqrt{1-t_j^2}} + \overline{K_2} \right) h + \epsilon \right). \end{aligned} \tag{11}$$

Proof see Appendix B.1.

This result shows that the first term in the bound scales the initial discrepancy $\mathcal{W}_2(\overleftarrow{P}_0, \overleftarrow{Q}_0)$ by the product of Lipschitz constants $\prod_{j=0}^{N-1} \mathrm{Lip}(\widetilde{T}_j)$, and the second term $\left(\overline{K}\sqrt{M_0} + \frac{\overline{K_1}}{\sqrt{1-t_j^2}} + \overline{K_2}\right)h + \epsilon$, captures accumulated

discretization errors (Assumption 5) and a local discretization error scales $\mathcal{O}(\sqrt{M_0})$, yielding the $\mathcal{O}(\sqrt{d})$ dependence in the isotropic case $C = I_d$. Similar results are listed in (Albergo & Vanden-Eijnden, 2023; Boffi et al., 2025), while the precise scaling of the second term remains unspecified. To be noted, in the limit of $h \to 0$, $h \sum_{k=0}^{N-2} \frac{1}{\sqrt{1-t_k^2}} \to \frac{\pi}{2}$.

Notably, Theorem 6 is of general validity: it applies to a general continuous flow matching generative model as long as its discrete counterparts satisfy the relevant assumptions; see also Appendix B.9, whose background coupling is not a Föllmer flow.

3.2 Analyses of Föllmer flow under Gaussian tail assumption

In this section, we focus on the Föllmer flow and derive the main convergence result based on Theorem 6 through Lipschitz changes of variables, which plays a central role in our analysis.

Assumption 7 (Third moment)**.** *The data distribution has a bounded third moment, i.e.* $\mathbb{E}_{p_0}|x|^3 < \infty$.

We note that the third-moment Assumption 7 is only required to ensure well-posedness of Föllmer flow at $t = 0$ in the proof of Lemma 11. For our complexity bound, the second moment Assumption 2 is sufficient.

Our analysis is based on the following key assumption that the tail distribution of the target is similar to a Gaussian distribution with covariance matrix A.

Assumption 8 (**Gaussian-tail**)**.** *The probability density function of target distribution* $\bar{p}_0 \in C^2(\mathbb{R}^d)$ *and admits the following tail decomposition:*

$$\bar{p}_0(x) = \exp\left(-\frac{|x|_A^2}{2}\right)\exp(h(x)), \tag{12}$$

where there are independent of dimension constants such that,

(i) A is a symmetric, positive-definite matrix which can be simultaneously diagonalized with C, and

$$\|A\| < \infty, \quad \|C\| < \infty, \quad \|AC^{-1}\| < \infty, \quad \|CA^{-1}\| < \infty.$$

(ii) the remainder term h follows

$$|\sqrt{C}\nabla h|_\infty < \infty, \quad \|C\nabla^2 h\|_\infty < \infty.$$

The Gaussian tail Assumption 8 generalizes the log-concavity condition in (Ding et al., 2023; Gao et al., 2024) to heavier-than-sub-Gaussian tails while ensuring sufficient decay for well-posedness and convergence. Although stronger than the weak semi-log-concavity assumption of (Chaintron et al., 2025; Bruno & Sabanis, 2025), it yields sharper complexity guarantees: the latter one implies $O(d)$ sampling complexity, whereas the Gaussian tail assumption achieves $O(\sqrt{d})$. Notably, the Gaussian tail Assumption 8 admits a non-log-concave setting and also accommodates realistic distributions such as early stopping and extendable to infinite-dimension; see Theorem 16, Theorem 20, and Theorem 25.

Similar Gaussian-tail-type decompositions of $\bar{p}_0$ in equation 12 also appeared in (Cole & Lu, 2024; Pidstrigach et al., 2024), primarily for establishing well-posedness and generalization of the sampling process. In contrast, our Assumption 8 is further tailored to analyze convergence of the discrete-time dynamics and its dimensional dependence; while slightly more restrictive, it ensures that the following theorem provides bounds on the Lipschitz constant and the time derivative of the Föllmer velocity field in equation 7. These bounds, in turn, support the Lipschitz change-of-variables argument in Corollary 12 and the convergence rate established in Theorem 16.

Theorem 9 (Regularity of the velocity field)**.** *The Gaussian tail Assumption 8 implies the Föllmer velocity field $V(t,\cdot)$ has the following regularity properties:* $\forall t \in [0,1]$,

$$\begin{aligned} |V(t,x)| &\le K_0 + K_2 t|x|, \\ \|\nabla V(t,\cdot)\|_\infty &\le (K_1 + K_2)t, \\ |\partial_t V(t,x)| &\le K_5|x| + \frac{K_6}{\sqrt{1-t^2}} + K_7, \end{aligned} \tag{13}$$

where the coefficients are dimension-free constants, given explicitly in Table 3 of Appendix C.

The quantity $|\partial_t V(1-t,x)|$, which characterizes the temporal variation of the score along the forward process, is commonly referred to as score perturbation bound (Chen et al., 2023b). Controlling this term is essential for convergence, as its local behaviour in the spatial and temporal domains may lead to instability. Existing works, therefore, combine time-domain restriction with early stopping to ensure sufficient regularity after a short amount of forward diffusion. For instance, to handle the blow-up of $|\partial_t V(t,x)|$ near $t = 0, 1$, Ding et al. (2023) restrict t to $[\delta, 1-\delta]$. In particular, Gao et al. (2024) shows Lipschitz continuity of V in t over $[0, 1-\delta_0]$ with constant scaling as $\mathcal{O}(\delta_0^{-2})$. In contrast, under our Gaussian tail assumption, the control over the second derivative of the tail allows us to bound $|\partial_t V(t,x)|$ using techniques such as the Brascamp-Lieb inequality (Brascamp & Lieb, 1976). Such analysis reveals that the temporal term $\frac{1}{\sqrt{1-t^2}}$ is integrable on $[0,1]$ and the spatial term is $\mathcal{O}(|x|)$. To our knowledge, it is the first to yield the improved $\mathcal{O}(\sqrt{d})$ complexity bound for the probability flow ODE in practice (without corrector terms if compared with (Chen et al., 2023b)); c.f. Corollary 17. Notably, this bound is dimensionless even in the presence of an anisotropic assumption ($C \neq I_d$), highlighting a qualitative improvement over prior analyses that rely on isotropic regularization or compact-support assumptions. Detailed proof of Theorem 9 is provided in Appendix B.2.

Remark 10. *Motivated by the averaged-velocity construction in MeanFlow (Geng et al., 2025), we introduce an analogous notion for the Föllmer flow and define the* averaged Föllmer velocity *as*

$$\overline{V}(x,r,t) := \frac{1}{t-r}\int_r^t V(\tau,x)\,d\tau.$$

Under the regularity condition equation 13 satisfied by the Föllmer velocity field, a direct calculation gives the uniform bound

$$\left|\overline{V}(x,r,t)\right| \;\leq\; K_0 \;+\; \frac{t+r}{2}\,K_2\,|x|,$$

demonstrating that the averaged Föllmer velocity preserves the same linear growth property as the original velocity field.

Under the preceding assumptions and analysis, we establish the well-posedness of the Föllmer model $(\overleftarrow{X}_t)_{t\in[0,1]}$ in the following lemma.

Lemma 11 (Well-posedness)**.** *Suppose that the third moment Assumption 7 and the Gaussian tail Assumption 8 hold. Then the Föllmer velocity field is well-defined at the $t = 0$, in the sense that*

$$V(0,x) := \lim_{t\to 0} V(t,x) = \lim_{t\to 0}\frac{x+S(t,x)}{t} = \sqrt{C}\mathbb{E}_{\bar{p}_0}[X]. \tag{14}$$

Consequently, the Föllmer flow $(\overleftarrow{X}_t)_{t\in[0,1]}$ is a unique solution to IVP equation 7. Moreover, the push-forward measure satisfies

$$\gamma_C \circ (\overleftarrow{X}_1)^{-1} = \bar{p}_0.$$

Proof see Appendix B.3.

Under Assumption 8, we now establish the Lipschitz property of the continuous flow $(\overleftarrow{X}_t)_{t\in[0,1]}$.

Corollary 12 (Lipschitzness of continuous flow)**.** *If $\bar{p}_0$ follows the Gaussian tail Assumption 8, then the Föllmer flow $(\overleftarrow{X}_t)_{t\in[0,1]}$ is Lipschitz with a dimension-free constant, more precisely,*

$$\mathrm{Lip}(\overleftarrow{X}_1(x)) \leq \|\nabla\overleftarrow{X}_1(x)\|_{op} \leq \exp\left(\frac{K_1+K_2}{2}\right). \tag{15}$$

Proof see Appendix B.4.

Bound like equation 15 can also be achieved in (Caffarelli, 2000; Colombo et al., 2017; Kim & Milman, 2012; Mikulincer & Shenfeld, 2023; Brigati & Pedrotti, 2024) under various assumptions, as detailed in Appendix A. In general, the constants involved are dimension-free.

To analyze the stability and convergence of the discrete flow, we first assume the following bound on the velocity field approximation error at the discretization points.

Assumption 13 (Accuracy of the learned velocity field)**.** *For each time discretization point t_n, the accuracy of learned velocity $\widetilde{V}(t_n, x)$ approximates the true velocity field $V(t_n, x)$ with uniformly bounded error in expectation:*

$$\mathbb{E}_{\overrightarrow{P}_{1-t_n}} |V(t_n, x) - \widetilde{V}(t_n, x)|^2 \leq \epsilon^2.$$

Next, we assume that the learned velocity field inherits the regularity of the continuous flow established in Theorem 9 under the Gaussian tail Assumption 8.

Assumption 14 (Regularity of the learned velocity field)**.** *Assume the learned velocity field $\widetilde{V}(t, x)$ follows*

$$\|\nabla \widetilde{V}(t_n, \cdot)\|_\infty \leq (K_1 + K_2 + K_8) t_n$$

for some positive constant K_8.

Assumption 14 can further be relaxed in the temporal t direction to require only that the total discrete-time sum of the score gradient is bounded; see Remark 23 in Appendix B.7. Such Lipschitz control over $\widetilde{V}$ is essential for our theoretical analysis and remains reasonable. The learned velocity field $\widetilde{V}(t_n, x)$ is trained to approximate the true velocity field $V(t_n, x)$ in Assumption 13, which satisfies the required regularity (see Theorem 9); moreover, neural networks may generally inherit the smoothness and controlled growth through training, and the Lipschitz property can also be enforced by employing spectral-normalized networks Miyato et al. (2018). We leave the question of the necessity of this Lipschitz control over $\widetilde{V}$ on the pathway to a $\sqrt{d}$-type optimal complexity bound open.

We subsequently establish the Lipschitz property of the discrete flow $(\overleftarrow{Y}_t)_{t\in[0,1]}$ under Assumption 14.

Corollary 15 (Lipschitzness of discrete flow)**.** *The regularity of learned velocity field Assumption 14 implies the Lipschitz property of the learned flow $(\overleftarrow{Y}_t)_{t\in[0,1]}$ with a dimension-free constant, such that*

$$\mathrm{Lip}(\overleftarrow{Y}_1(x)) \leq \|\nabla \overleftarrow{Y}_1(x)\|_{op} \leq \exp\left(\frac{K_1 + K_2 + K_8}{2}\right).$$

Proof see Appendix B.5.

3.3 Main Convergence theories

With the Lipschitz properties of the flow established (see Corollary 12 and Corollary 15), we next quantify how these bounds propagate through the discrete dynamics. Building on Theorem 6, the following theorem provides a convergence result in Föllmer flow case.

Theorem 16. *Suppose that the third moment Assumption 7, the Gaussian tail Assumption 8, the accuracy and regularity assumptions 13- 14 on the learned velocity field hold. Using the Euler method for the Föllmer flow with uniform step size $h = t_{n+1} - t_n \leq 1$ ensures $\sqrt{M_0}$ convergence between the target data distribution and the generated distribution:*

$$\mathcal{W}_2(\overrightarrow{P}_0, \overleftarrow{Q}_1) \leq \exp\left(\frac{K_1 + K_2 + K_8}{2}\right)\left(\sqrt{3}\left(K_5\sqrt{M_0} + K_9\right)h + 2\epsilon\right). \tag{16}$$

where $K_1, K_2, \ldots, K_9$ are dimensionless constants defined in Theorem 9 and Assumption 14, with explicit expressions given in Table 3 of Appendix C. Furthermore, with the covariance of base distribution $C = I_d$ in the Assumption 2, $\mathcal{W}_2(\overrightarrow{P}_0, \overleftarrow{Q}_1) = \mathcal{O}(\sqrt{d}\,h + \epsilon)$.

Proof see Appendix B.6.

Corollary 17. *To reach a distribution $\overleftarrow{Q}_1$ such that $\mathcal{W}_2(\overrightarrow{P}_0, \overleftarrow{Q}_1) = \mathcal{O}(\varepsilon_0)$ with uniform step size $h = t_{n+1} - t_n \leq 1$ requires at most:*

$$h = \mathcal{O}\left(\frac{\epsilon_0}{\sqrt{M_0}}\right), \quad N = \frac{1}{h} = \mathcal{O}\left(\frac{\sqrt{M_0}}{\epsilon_0}\right),$$

and Assumption 13 to hold with $\epsilon = \mathcal{O}(\epsilon_0)$. Furthermore, $N = \mathcal{O}\left(\frac{\sqrt{d}}{\epsilon_0}\right)$ under the Assumption 2 with $C = I_d$.

The complexity bound established in Corollary 17 grows linearly with the square root of the trace of the forward process's covariance operator, independent of dimension, and thus extends naturally to infinite-dimensional generative models. An illustrative case is provided in Appendix B.10, where we consider Bayesian inverse problems in function spaces. Moreover, under the normalized case ($C = I_d$), our N scales like $\sqrt{d}$, which is shown to be optimal in Proposition 6 of (Gao et al., 2025). Since the probabilistic ODE (Prob ODE) (Song et al., 2021; Gao & Zhu, 2025) can be viewed as a time-rescaled Föllmer flow, the result of Corollary 17 also implies that our method improves the computational complexity of the Prob ODE compared to (Wang & Wang, 2024). We will provide a detailed discussion in Appendix B.8. The result of Corollary 17 indicates that our method improves the computational complexity of the Prob ODE, whereas (Wang & Wang, 2024) shows $N = \mathcal{O}\left(\frac{M_0}{\epsilon_0^2}\left(\log \frac{M_2 + \mathrm{Tr}(C)}{\epsilon_0^2}\right)^3\right)$ under the same setting.

We further verified that our method extends to the 1-rectified flow setting (Liu et al., 2023; Rout et al., 2024). In particular, it applies to the interpolation paths used in the flow built by the first step rectification over independent coupling prior to the recursive construction, and retains the same $\mathcal{O}(\sqrt{d})$ complexity stated in Corollary 17. The proof is deferred to Appendix B.9.

3.4 Convergence under bounded-support assumption

Real-world data often lie on low-dimensional manifolds, where the distribution is not absolutely continuous with respect to Lebesgue measure in the ambient dimension, and therefore KL bounds may diverge (Pidstrigach, 2022). This motivates the adoption and study of the manifold assumption (De Bortoli, 2022; Yubin et al., 2025), which, under compactness, entails the following bounded-support assumption.

Assumption 18 (Bounded-support assumption)**.** *Suppose distribution p_0 has compact support with* $\mathrm{Diam}(\mathrm{Supp}(p_0)) \leq R$ *for some constant $R > 0$.*

Let $q_\sigma = \exp\left(-\frac{|x|^2}{2\sigma^2}\right) * q_0$, where q_0 satisfies the bounded-support Assumption 18. Consider $g(x) = \log q_\sigma(x) + \frac{|x|^2}{2\sigma^2}$, inspired by similar results in (De Bortoli, 2022; Mooney et al., 2025; Wang & Wang, 2024), we have

$$|\nabla g|_\infty \leq \frac{R}{\sigma^2}, \quad \|\nabla^2 g\|_\infty \leq \frac{2R^2}{\sigma^4}. \tag{17}$$

Set $0 = t_0 < t_1 < \cdots < t_N = 1 - \delta$ as the discretization points, where the early stopping (Lyu et al., 2022) coefficient $\delta \ll 1$. By expressing the distribution of the forward process of Föllmer flow at stopping time δ in the form q_σ, we obtain the correspondences

$$\sigma^2 \longleftrightarrow 1 - (1-\delta)^2, \quad q_0(x) \longleftrightarrow \frac{1}{1-\delta}\overrightarrow{P}_0\left(\frac{1}{1-\delta}x\right).$$

Then by Theorem 9, we get the following Lipschitz bound of the velocity field under Assumption 18.

Corollary 19. *Suppose that the bounded-support Assumption 18 holds. Taking $C = I_d$ in equation 7, and $A = (1-(1-\delta)^2)I_d$ in Assumption 8, then for all $t \in [0, 1-\delta]$,*

$$\begin{aligned} |V(t,x)| &\leq K_0^* + K_2^* t|x|, \\ \|\nabla V(t,\cdot)\|_\infty &\leq (K_1^* + K_2^*)t, \\ |\partial_t V(t,x)| &\leq K_5^*|x| + \frac{K_6^*}{\sqrt{1-t^2}} + K_7^*, \end{aligned}$$

where coefficients are defined in Table 5 of Appendix C.

The proof parallels the corollary in (Wang & Wang, 2024). Using the Lipschitz bound from Corollary 19, we obtain a bounded-support-version W_2 bound by tracking the constants in Theorem 16.

Theorem 20. *Suppose that the bounded-support Assumption 18 and the accuracy and regularity Assumptions 13, 14 hold. Take $C = I_d$, $\delta \ll 1$, then we have*

$$\mathcal{W}_2(\overrightarrow{P}_\delta, \overleftarrow{Q}_{1-\delta}) \leq \exp\left(\frac{3R^2}{2\delta^2} + \frac{1}{2\delta} + \frac{K_8}{2}\right)\left(\sqrt{3}\left(K_5^*\sqrt{M_0} + K_9^*\right)h + 2\epsilon\right),$$

where K_5^* and K_9^* are dimension-free constants, whose explicit forms given in Table 5 of Appendix C, and the constant K_8 is defined in Assumption 14.

With the result in Theorem 20, we can directly compute the complexity bound under the bounded-support assumption with early stopping technique.

Corollary 21. *With R and δ fixed, achieving a distribution $\overleftarrow{Q}_{1-\delta}$ such that $\mathcal{W}_2(\overrightarrow{P}_\delta, \overleftarrow{Q}_{1-\delta}) = \mathcal{O}(\epsilon_0)$ requires at most: $N = \mathcal{O}\left(\frac{\sqrt{d}}{\epsilon_0}\right)$, and Assumption 13 to hold with $\epsilon = \mathcal{O}(\epsilon_0)$.*

Noticing that,

$$\mathcal{W}_2(\overrightarrow{P}_\delta, \overrightarrow{P}_0) \leq \sqrt{\mathbb{E}|\overrightarrow{X}_\delta - \overrightarrow{X}_0|^2} \leq \sqrt{2d\delta},$$

the complexity bound can also be derived with respect to $\overrightarrow{P}_0$. More precisely, we consider the following practical scenario. Now we assume $R^2 = \mathcal{O}(d)$, then optimizing δ to achieve $\mathcal{W}_2(\overrightarrow{P}_0, \overleftarrow{Q}_{1-\delta}) = \mathcal{O}(\epsilon_0)$ requires at most logarithmic complexity with $\log N = \mathcal{O}\left(\frac{d^3}{\epsilon_0^4}\right)$.

3.5 Numerical Illustration

We validate the optimal $\mathcal{O}(\sqrt{d})$ complexity bound in Theorem 16 through controlled numerical experiments. To this end, we consider a synthetic distribution for which both the Gaussian-tail constants in Assumption 8 and the associated Föllmer velocity field can be computed explicitly. Specifically, the d-dimensional target distribution is chosen as the Gaussian mixture

$$p_{\text{data}}(x) = \frac{1}{2}\exp\left(-\frac{|x-a|^2}{2\tau}\right) + \frac{1}{2}\exp\left(-\frac{|x+a|^2}{2\tau}\right), \tag{18}$$

where $a \in \mathbb{R}^d$ and $\tau > 0$. This distribution admits the Gaussian-tail decomposition

$$p_{\text{data}}(x) = \exp\left(-\frac{|x|^2}{2\tau}\right)\exp(h(x)),$$

with

$$h(x) = \log\left(\exp\left(-\frac{|a|^2}{2\tau} + \frac{\langle a, x\rangle}{\tau}\right) + \exp\left(-\frac{|a|^2}{2\tau} - \frac{\langle a, x\rangle}{\tau}\right)\right).$$

A direct calculation shows that $\nabla h(x) = \tanh\left(\frac{\langle a,x\rangle}{\tau}\right)\frac{a}{\tau}$, and hence $\|\nabla h\|_\infty$ remains uniformly bounded provided $|a|_2$ is dimension-independent. Similarly, the Hessian satisfies $\sup_x \|\nabla^2 h(x)\|_2 \leq \frac{|a|_2^2}{\tau^2}$, which implies that both first- and second-order derivatives are uniformly bounded in d. Therefore, the Gaussian-tail Assumption 8 holds with dimension-free constants. In the experiments, we fix $a = (1, 0, \ldots, 0)^\top$.

Under this setting, the score function and the corresponding Föllmer velocity field admit closed-form expressions with

$$\begin{aligned} V(t,x) =& \frac{1}{t}\left[x + S(t,x)\right] \\ =& \frac{1}{t}\left[x + C\nabla\log\left(\frac{1}{2}\exp\left(-\frac{|x-ta|^2_{\bar{A}_t}}{2}\right) + \frac{1}{2}\exp\left(-\frac{|x+ta|^2_{\bar{A}_t}}{2}\right)\right)\right] \end{aligned}$$

$$=\frac{1}{t}\Big[(I - C\bar{A}_t^{-1})x + tC\bar{A}_t^{-1}a\tanh\big(t\cdot a^\top \bar{A}_t^{-1}x\big)\Big],$$

allowing us to simulate an ideal Föllmer flow sampler. We measure the discretization error via the coupled estimator $\left(\frac{1}{M}\sum_{i=1}^{M}\|X^{(i)} - Y^{(i)}\|^2\right)^{1/2}$, which upper bounds the Wasserstein distance in Theorem 16.

Time discretization. We first study the dependence on the time step size h in dimension $d = 50$. The initial particles are sampled from $X_0 \sim \mathcal{N}(0, I_d)$ with $M = 2000$, and we consider step numbers $N \in \{20, 40, 80, 160, 320, 640\}$. Figure 1a shows the error in log–log scale as a function of h. The fitted slope is approximately 0.955, which is consistent with the first-order convergence rate predicted by Theorem 16.

Dimension scaling. We next examine the dependence on the dimension $d \in \{5, 10, 20, 40, 80, 160, 320, 640\}$. For each d, we determine the minimal number of Euler steps N required to achieve a fixed tolerance $\varepsilon_0 = 10^{-2}$, using a reference solution with $N_{\text{ref}} = 50000$. The resulting scaling, shown in Figure 1b, satisfies $N(d) \propto d^{0.472}$, which is in strong agreement with the theoretical $\mathcal{O}(\sqrt{d})$ complexity.

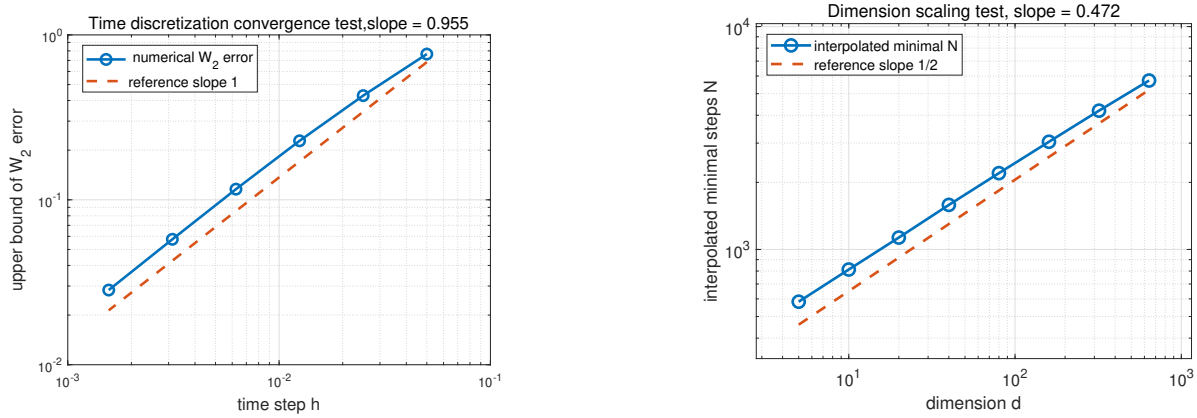

(a) Time discretization

(b) Dimension scaling

Figure 1: Numerical validation of Euler discretization.

4 Conclusion and Future Directions

We establish an optimal $\mathcal{O}(\sqrt{\operatorname{Tr} C})$ ($\mathcal{O}(\sqrt{d})$) complexity bound for flow-based generative models under the Wasserstein metric via dimension-free Lipschitz control of truncation errors. The result applies to Föllmer and 1-rectified flows under a Gaussian-tail assumption, extending to bounded-support and infinite-dimensional settings. Numerical results confirm first-order convergence and the predicted scaling.

Several directions merit further investigation:

- **Beyond Gaussian tails.** Weak log-concavity (Bruno & Sabanis, 2025; Gentiloni-Silveri & Ocello, 2025) extends the Gaussian-tail assumption, but current results only achieve $\mathcal{O}(d)$ complexity. Whether the optimal $\mathcal{O}(\sqrt{d})$ rate persists under this broader condition remains open.
- **Higher-order integrators.** Extending the analysis to higher-order schemes requires refined regularity assumptions (e.g., higher-order time derivatives). Identifying minimal conditions for higher-order Wasserstein convergence is an important direction.
- **Error control and algorithmic design.** Understanding how training objectives, temporal reweighting, and adaptive sampling interact with step-size design (especially under the singular behavior $\frac{1}{\sqrt{1-t^2}}$), and developing data-driven estimates of Lipschitz constants, may lead to sharper Wasserstein error bounds and improved practical performance.

References

Josh Achiam, Steven Adler, Sandhini Agarwal, Lama Ahmad, Ilge Akkaya, Florencia Leoni Aleman, Diogo Almeida, Janko Altenschmidt, Sam Altman, Shyamal Anadkat, et al. Gpt-4 technical report. *arXiv preprint arXiv:2303.08774*, 2023.

Michael S Albergo, Nicholas M Boffi, and Eric Vanden-Eijnden. Stochastic interpolants: A unifying framework for flows and diffusions. *arXiv preprint arXiv:2303.08797*, 2023.

Michael Samuel Albergo and Eric Vanden-Eijnden. Building normalizing flows with stochastic interpolants. In *The Eleventh International Conference on Learning Representations*, 2023. URL `https://openreview.net/forum?id=li7qeBbCR1t`.

Luigi Ambrosio and Gianluca Crippa. Continuity equations and ODE flows with non-smooth velocity. *Proceedings of the Royal Society of Edinburgh Section A: Mathematics*, 144(6):1191–1244, 2014.

Martin Arjovsky, Soumith Chintala, and Léon Bottou. Wasserstein generative adversarial networks. In *International conference on machine learning*, pp. 214–223. PMLR, 2017.

Cesare Arzela. *Sulle funzioni di linee*. Gamberini e Parmeggiani, 1895.

Georgios Batzolis, Jan Stanczuk, Carola-Bibiane Schönlieb, and Christian Etmann. Conditional image generation with score-based diffusion models. *arXiv preprint arXiv:2111.13606*, 2021.

Yoshua Bengio, Ian Goodfellow, Aaron Courville, et al. *Deep learning*, volume 1. MIT press Cambridge, MA, USA, 2017.

Joe Benton, Valentin De Bortoli, Arnaud Doucet, and George Deligiannidis. Nearly d-linear convergence bounds for diffusion models via stochastic localization. In *The Twelfth International Conference on Learning Representations*, 2024. URL `https://openreview.net/forum?id=r5njV3BsuD`.

Nicholas Matthew Boffi, Michael Samuel Albergo, and Eric Vanden-Eijnden. Flow map matching with stochastic interpolants: A mathematical framework for consistency models. *Transactions on Machine Learning Research*, 2025.

Herm Jan Brascamp and Elliott H Lieb. On extensions of the brunn-minkowski and prékopa-leindler theorems, including inequalities for log concave functions, and with an application to the diffusion equation. *Journal of functional analysis*, 22(4):366–389, 1976.

Giovanni Brigati and Francesco Pedrotti. Heat flow, log-concavity, and lipschitz transport maps. *arXiv preprint arXiv:2404.15205*, 2024.

Stefano Bruno and Sotirios Sabanis. Wasserstein convergence of score-based generative models under semi-convexity and discontinuous gradients. *Transactions on Machine Learning Research*, 2025. ISSN 2835-8856. URL `https://openreview.net/forum?id=vS9iVRB7XF`.

Luis A Caffarelli. Monotonicity properties of optimal transportation and the fkg and related inequalities. *Communications in Mathematical Physics*, 214(3):547–563, 2000.

Louis-Pierre Chaintron, Giovanni Conforti, and Katharina Eichinger. Propagation of weak log-concavity along generalised heat flows via hamilton-jacobi equations. *arXiv preprint arXiv:2508.07931*, 2025.

Hongrui Chen, Holden Lee, and Jianfeng Lu. Improved analysis of score-based generative modeling: User-friendly bounds under minimal smoothness assumptions. In *International Conference on Machine Learning*, pp. 4735–4763. PMLR, 2023a.

Ricky TQ Chen, Yulia Rubanova, Jesse Bettencourt, and David K Duvenaud. Neural ordinary differential equations. *Advances in neural information processing systems*, 31, 2018.

Sitan Chen, Sinho Chewi, Holden Lee, Yuanzhi Li, Jianfeng Lu, and Adil Salim. The probability flow ode is provably fast. *Advances in Neural Information Processing Systems*, 36:68552–68575, 2023b.

Sitan Chen, Giannis Daras, and Alex Dimakis. Restoration-degradation beyond linear diffusions: A non-asymptotic analysis for ddim-type samplers. In *International Conference on Machine Learning*, pp. 4462–4484. PMLR, 2023c.

Xiuyuan Cheng, Jianfeng Lu, Yixin Tan, and Yao Xie. Convergence of flow-based generative models via proximal gradient descent in wasserstein space. *IEEE Transactions on Information Theory*, 70(11):8087–8106, 2024.

Frank Cole and Yulong Lu. Score-based generative models break the curse of dimensionality in learning a family of sub-gaussian probability distributions. In *12th International Conference on Learning Representations, ICLR 2024*, 2024.

Maria Colombo, Alessio Figalli, and Yash Jhaveri. Lipschitz changes of variables between perturbations of log-concave measures. *Annali Della Scuola Normale Superiore Di Pisa-Classe Di Scienze*, 17(4):1491–1519, 2017.

Giovanni Conforti. Weak semiconvexity estimates for schrödinger potentials and logarithmic sobolev inequality for schrödinger bridges. *Probability Theory and Related Fields*, 189(3):1045–1071, 2024.

Giovanni Conforti, Alain Durmus, and Marta Gentiloni Silveri. KL convergence guarantees for score diffusion models under minimal data assumptions. *SIAM Journal on Mathematics of Data Science*, 7(1):86–109, 2025a.

Giovanni Conforti, Daniel Lacker, and Soumik Pal. Projected langevin dynamics and a gradient flow for entropic optimal transport. *Journal of the European Mathematical Society*, 2025b.

Yin Dai, Yuan Gao, Jian Huang, Yuling Jiao, Lican Kang, and Jin Liu. Lipschitz transport maps via the Föllmer flow. *arXiv preprint arXiv:2309.03490*, 2023.

Valentin De Bortoli. Convergence of denoising diffusion models under the manifold hypothesis. *Transactions on Machine Learning Research*, 2022. ISSN 2835-8856. URL `https://openreview.net/forum?id=MhK5aXo3gB`.

Zhao Ding, Yuling Jiao, Xiliang Lu, Zhijian Yang, and Cheng Yuan. Sampling via Föllmer flow. *arXiv preprint arXiv:2311.03660*, 2023.

Max Fathi, Dan Mikulincer, and Yair Shenfeld. Transportation onto log-lipschitz perturbations. *Calculus of Variations and Partial Differential Equations*, 63(3):61, 2024.

Xuefeng Gao and Lingjiong Zhu. Convergence analysis for general probability flow ODEs of diffusion models in wasserstein distances. In *28th International Conference on Artificial Intelligence and Statistics (AISTATS)*, volume 258, 2025.

Xuefeng Gao, Hoang M Nguyen, and Lingjiong Zhu. Wasserstein convergence guarantees for a general class of score-based generative models. *Journal of machine learning research*, 26(43):1–54, 2025.

Yuan Gao, Jian Huang, Yuling Jiao, and Shurong Zheng. Convergence of continuous normalizing flows for learning probability distributions. *Machine Learning*, 2024.

Zhengyang Geng, Mingyang Deng, Xingjian Bai, J Zico Kolter, and Kaiming He. Mean flows for one-step generative modeling. *arXiv preprint arXiv:2505.13447*, 2025.

Marta Gentiloni-Silveri and Antonio Ocello. Beyond log-concavity and score regularity: Improved convergence bounds for score-based generative models in w2-distance. *arXiv preprint arXiv:2501.02298*, 2025.

Ian Goodfellow, Jean Pouget-Abadie, Mehdi Mirza, Bing Xu, David Warde-Farley, Sherjil Ozair, Aaron Courville, and Yoshua Bengio. Generative adversarial nets. In *Advances in Neural Information Processing Systems*, volume 27. Curran Associates, Inc., 2014.

Young-Heon Kim and Emanuel Milman. A generalization of caffarelli's contraction theorem via (reverse) heat flow. *Mathematische Annalen*, 354(3):827–862, 2012.

Diederik P. Kingma and Max Welling. Auto-encoding variational bayes. In *2nd International Conference on Learning Representations*, 2014.

Diederik P Kingma, Max Welling, et al. An introduction to variational autoencoders. *Foundations and Trends® in Machine Learning*, 12(4):307–392, 2019.

Christian Léonard. A survey of the schrödinger problem and some of its connections with optimal transport. *Discrete and Continuous Dynamical Systems*, 34, 2013. doi: 10.3934/dcds.2014.34.1533.

Gen Li, Yu Huang, Timofey Efimov, Yuting Wei, Yuejie Chi, and Yuxin Chen. Accelerating convergence of score-based diffusion models, provably. In *Forty-first International Conference on Machine Learning*, 2024. URL https://openreview.net/forum?id=KB6slOUQP9.

Jae Hyun Lim, Nikola B Kovachki, Ricardo Baptista, Christopher Beckham, Kamyar Azizzadenesheli, Jean Kossaifi, Vikram Voleti, Jiaming Song, Karsten Kreis, Jan Kautz, et al. Score-based diffusion models in function space. *Journal of Machine Learning Research*, 26(158):1–62, 2025.

Yaron Lipman, Ricky T. Q. Chen, Heli Ben-Hamu, Maximilian Nickel, and Matthew Le. Flow matching for generative modeling. In *The Eleventh International Conference on Learning Representations*, 2023. URL https://openreview.net/forum?id=PqvMRDCJT9t.

Xingchao Liu, Chengyue Gong, and qiang liu. Flow straight and fast: Learning to generate and transfer data with rectified flow. In *The Eleventh International Conference on Learning Representations*, 2023. URL https://openreview.net/forum?id=XVjTT1nw5z.

Zhaoyang Lyu, Xudong Xu, Ceyuan Yang, Dahua Lin, and Bo Dai. Accelerating diffusion models via early stop of the diffusion process. *arXiv preprint arXiv:2205.12524*, 2022.

Dan Mikulincer and Yair Shenfeld. On the lipschitz properties of transportation along heat flows. In *Geometric Aspects of Functional Analysis: Israel Seminar (GAFA) 2020-2022*, pp. 269–290. Springer, 2023.

Takeru Miyato, Toshiki Kataoka, Masanori Koyama, and Yuichi Yoshida. Spectral normalization for generative adversarial networks. *arXiv preprint arXiv:1802.05957*, 2018.

Connor Mooney, Zhongjian Wang, Jack Xin, and Yifeng Yu. Global well-posedness and convergence analysis of score-based generative models via sharp lipschitz estimates. In *The Thirteenth International Conference on Learning Representations*, 2025. URL https://openreview.net/forum?id=r3cWq6KKbt.

Joe Neeman. Lipschitz changes of variables via heat flow. *arXiv preprint arXiv:2201.03403*, 2022.

George Papamakarios, Eric Nalisnick, Danilo Jimenez Rezende, Shakir Mohamed, and Balaji Lakshminarayanan. Normalizing flows for probabilistic modeling and inference. *Journal of Machine Learning Research*, 22(57):1–64, 2021.

Jakiw Pidstrigach. Score-based generative models detect manifolds. *Advances in Neural Information Processing Systems*, 35:35852–35865, 2022.

Jakiw Pidstrigach, Youssef Marzouk, Sebastian Reich, and Sven Wang. Infinite-dimensional diffusion models. *Journal of Machine Learning Research*, 25(414):1–52, 2024.

Litu Rout, Yujia Chen, Nataniel Ruiz, Constantine Caramanis, Sanjay Shakkottai, and Wen-Sheng Chu. Semantic image inversion and editing using rectified stochastic differential equations. *arXiv preprint arXiv:2410.10792*, 2024.

Tim Salimans and Jonathan Ho. Progressive distillation for fast sampling of diffusion models. In *International Conference on Learning Representations*, 2022. URL https://openreview.net/forum?id=TIdIXIpzhoI.

Yang Song, Jascha Sohl-Dickstein, Diederik P Kingma, Abhishek Kumar, Stefano Ermon, and Ben Poole. Score-based generative modeling through stochastic differential equations. In *International Conference on Learning Representations*, 2021. URL `https://openreview.net/forum?id=PxTIG12RRHS`.

Joshua B Tenenbaum, Vin de Silva, and John C Langford. A global geometric framework for nonlinear dimensionality reduction. *science*, 290(5500):2319–2323, 2000.

Rens van de Schoot, Sarah Depaoli, Ruth King, Bianca Kramer, Kaspar Märtens, Mahlet G Tadesse, Marina Vannucci, Andrew Gelman, Duco Veen, Joukje Willemsen, et al. Bayesian statistics and modelling. *Nature Reviews Methods Primers*, 1(1):1, 2021.

Xiaoliang Wan and Shuangqing Wei. Vae-krnet and its applications to variational bayes. *Communications in Computational Physics*, 31(4):1049–1082, 2022.

Hanchen Wang, Tianfan Fu, Yuanqi Du, Wenhao Gao, Kexin Huang, Ziming Liu, Payal Chandak, Shengchao Liu, Peter Van Katwyk, Andreea Deac, et al. Scientific discovery in the age of artificial intelligence. *Nature*, 620(7972):47–60, 2023.

Xixian Wang and Zhongjian Wang. Wasserstein bounds for generative diffusion models with gaussian tail targets. *arXiv preprint arXiv:2412.11251*, 2024.

Lu Yubin, Wang Zhongjian, and Bal Guillaume. Mathematical analysis of singularities in the diffusion model under the submanifold assumption. *East Asian Journal on Applied Mathematics*, 15(4):669–700, 2025.

Appendix

A Comparison of Lipschitz Bounds via Heat Flow

In this appendix section, we summarize several related results from the literature and compare them with the estimate obtained in this work.

Table 2: Lip changes of variables via Heat flow

Target P_0	**Lip-constant**	**Result**
log-concave+sym.Ass.	1+sym.Ass.	Kim & Milman (2012)
κ-log-concave+osc $\leq c$	$2(2\kappa)^{e^c}$	Neeman (2022) Thm. 1.3
κ-log-concave	$e^{\frac{1-\kappa D^2}{2}} D$	Mikulincer & Shenfeld (2023) Thm. 1
κ-log-concave + L-log-Lipschitz perturbation	$\frac{1}{\sqrt{\kappa}} e^{\left(\frac{L^2}{2\kappa}+2\frac{L}{\sqrt{\kappa}}\right)}$	Brigati & Pedrotti (2024) Thm. 1.4
G-tail Ass. 8	$\frac{1}{\sqrt{\kappa}} e^{\left(\frac{L^2+L_1}{2\kappa}\right)}$	This work Cor. 22

where $\kappa, c, D, L, L_1, K_1, K_2$ are dimension-independent constant.

Corollary 22 (This work Cor. 12 with $A = (\kappa I_d)^{-1}$ and $C = I_d$)**.** *Let $\mu = e^{-(W(x)-H(x))}$ be a probability density on $\mathbb{R}^d$ such that $W(x) = \frac{\kappa|x|^2}{2}$ while $H(x)$ being L-Lipschitz and $\|\nabla^2 H\|_\infty < L_1$ for some $L, L_1 \geq 0$. Then, there exists a map $T^{\text{flow}} : \mathbb{R}^d \to \mathbb{R}^d$ such that $(T^{\text{flow}})_\# \gamma_d = \mu$ and T^{flow} is $\frac{1}{\sqrt{\kappa}} \exp\left(\frac{L^2+L_1}{2\kappa}\right)$-Lipschitz.*

Sketch of calculation. Applying Cor. 12 with $A = (\kappa I_d)^{-1}$ and $C = I_d$, Both A and C are diagonalizable, which leads to a more refined Lip upper bound:

$$\begin{aligned}
&\exp\left(\int_0^1 \frac{\|A\|^2(L^2+L_1)t}{(\|A\|t^2+\|C\|(1-t^2))^2}\,dt + \int_0^1 \frac{\|A-C\|t}{\|A\|t^2+\|C\|(1-t^2)}\,dt\right) \\
\leq &\exp\left(\frac{\|A\|(L^2+L_1)}{2\|C\|} + \frac{1}{2}\ln\frac{\|A\|}{\|C\|}\right) \leq \frac{1}{\sqrt{\kappa}}\exp\left(\frac{L^2+L_1}{2\kappa}\right).
\end{aligned}$$

□

B Proofs

In this part, we provide the detailed proofs of the theories in this paper.

B.1 Proof of Theorem 6

Proof. Recall the p-Wasserstein distance

$$\mathcal{W}_p(\mu,\nu) := \Big(\inf_{\gamma\in\Gamma(\mu,\nu)} \mathbb{E}_{(x,y)\sim\gamma}[\|x-y\|^p]\Big)^{1/p},$$

where $\Gamma(\mu,\nu)$ denotes the set of couplings with marginals μ and ν.

By the push-forward relation equation 3, pushing the coupling $\overleftarrow{Q}_{t_n}$ and $\overleftarrow{P}_{t_n}$ forward through the transport maps $\widetilde{T}_n$ and T_n yields a coupling of $\overleftarrow{Q}_{t_{n+1}}$ and $\overleftarrow{P}_{t_{n+1}}$, which gives

$$
\begin{aligned}
&\mathcal{W}_2(\overleftarrow{P}_{t_{n+1}}, \overleftarrow{Q}_{t_{n+1}}) \\
\leq &\sqrt{\mathbb{E}_{(\overleftarrow{Y}_{t_n}, \overleftarrow{X}_{t_n}) \sim \Gamma(\overleftarrow{Q}_{t_n}, \overleftarrow{P}_{t_n})} |\widetilde{T}_n(\overleftarrow{Y}_{t_n}) - T_n(\overleftarrow{X}_{t_n})|^2} \\
\leq &\sqrt{\mathbb{E}_{(\overleftarrow{Y}_{t_n}, \overleftarrow{X}_{t_n}) \sim \Gamma(\overleftarrow{Q}_{t_n}, \overleftarrow{P}_{t_n})} |\widetilde{T}_n(\overleftarrow{Y}_{t_n}) - \widetilde{T}_n(\overleftarrow{X}_{t_n})|^2} + \sqrt{\mathbb{E}_{\overleftarrow{X}_{t_n} \sim \overleftarrow{P}_{t_n}} |\widetilde{T}_n(\overleftarrow{X}_{t_n}) - T_n(\overleftarrow{X}_{t_n})|^2} \\
\leq &\mathrm{Lip}(\widetilde{T}_n) \sqrt{\mathbb{E}_{(\overleftarrow{Y}_{t_{n-1}}, \overleftarrow{X}_{t_{n-1}}) \sim \Gamma(\overleftarrow{Q}_{t_{n-1}}, \overleftarrow{P}_{t_{n-1}})} |\widetilde{T}_{n-1}(\overleftarrow{Y}_{t_{n-1}}) - \widetilde{T}_{n-1}(\overleftarrow{X}_{t_{n-1}})|^2} \\
&+ h\left(\left(\overline{K}\sqrt{M_0} + \frac{\overline{K_1}}{\sqrt{1-t_n^2}} + \overline{K_2}\right)h + \epsilon\right),
\end{aligned}
$$

where the last inequality uses Assumption 4 and Assumption 5. Then applying the discrete Grönwall inequality yields equation 11. □

B.2 Proof of Theorem 9

Proof. For simplicity, denote

$$
\begin{aligned}
G(t,x,y) &:= \exp\left(-\frac{\left|K(t)(\sqrt{C})^{-1}x - y\right|_{B(t)}^2}{2}\right), \\
g(t,x,y) &:= \partial_t \left(-\frac{\left|K(t)(\sqrt{C})^{-1}x - y\right|_{B(t)}^2}{2}\right).
\end{aligned} \tag{19}
$$

Under the Gaussian tail Assumption 8, the score function of Föllmer flow can be calculated by

$$
\begin{aligned}
S(t,x) :=& C\nabla \log p_t \\
=& C\nabla \log \int_{\mathbb{R}^d} \left(2\pi \det\big(B(t)\big)\right)^{-\frac{d}{2}} G(t,x,y) \cdot \exp\left(-\frac{|x|_{\overline{A}_t}^2}{2}\right) \exp\Big(h(\sqrt{C}y)\Big)\, \mathrm{d}y,
\end{aligned} \tag{20}
$$

where $\overline{A}_t = At^2 + C(1-t^2)$, $K(t) = (A\overline{A}_t^{-1})t$, $B(t) = (A\overline{A}_t^{-1})(1-t^2)$.

First, we consider the modified score function over the time interval $(0,1]$,

$$
\begin{aligned}
\widetilde{S}(t,x) &= S(t,x) + C\overline{A}_t^{-1}x \\
&= C\nabla \log \int_{\mathbb{R}^d} \big(2\pi B(t)\big)^{-\frac{d}{2}} G(t,x,y) \exp\Big(h(\sqrt{C}y)\Big)\, \mathrm{d}y \\
&= C\frac{\int_{\mathbb{R}^d} \nabla_x G(t,x,y) \exp\Big(h(\sqrt{C}y)\Big)\, \mathrm{d}y}{\int_{\mathbb{R}^d} G(t,x,y) \exp\Big(h(\sqrt{C}y)\Big)\, \mathrm{d}y} \\
&= -\frac{K(t)\sqrt{C}\int_{\mathbb{R}^d} \nabla_y G(t,x,y) \exp\Big(h(\sqrt{C}y)\Big)\, \mathrm{d}y}{\int_{\mathbb{R}^d} G(t,x,y) \exp\Big(h(\sqrt{C}y)\Big)\, \mathrm{d}y}
\end{aligned} \tag{21}
$$

$$= \frac{K(t)\sqrt{C}\int_{\mathbb{R}^d} G(t,x,y)\nabla_y h(\sqrt{C}y)\exp\left(h(\sqrt{C}y)\right)\mathrm{d}y}{\int_{\mathbb{R}^d} G(t,x,y)\exp\left(h(\sqrt{C}y)\right)\mathrm{d}y},$$

Here, the last equal sign is derived from integration by parts.

Since $G(t,x,y)\exp\left(h(\sqrt{C}y)\right) \geq 0$,

$$|\widetilde{S}(t,x)| \leq |K(t)\sqrt{C}\nabla h(\sqrt{C}x)|.$$

Let $K = \sup_{0\leq t\leq 1}|\frac{1}{t}K(t)| = \sup_{0\leq t\leq 1}|A\bar{A}_t^{-1}| \leq \max\{1, \|AC^{-1}\|\}$, we have

$$|\widetilde{S}(t,\cdot)| \leq K\|C\|^{1/2}|\sqrt{C}\nabla h|_\infty t = K_0 t.$$

Taking the derivative twice along that direction and using the same method as above, we get :

$$\|\nabla\widetilde{S}(t,\cdot)\|_\infty \leq K(t)^2(\|C\nabla^2 h\|_\infty + |\sqrt{C}\nabla h|_\infty^2) = K_1 t^2.$$

where $K_1 := K^2(\|C\nabla^2 h\|_\infty + |\sqrt{C}\nabla h|_\infty^2)$.

Define $K_2 := \sup_{0\leq t\leq 1}\|\frac{1}{t^2}(I - C\bar{A}_t^{-1})\| = \sup_{0\leq t\leq 1}\|(A-C)(At^2 + C(1-t^2))^{-1}\|$, then $\|(I - C\bar{A}_t^{-1})\| \leq K_2 t^2$.

Recall definition of $V(t,x)$ in equation 7, we have

$$|V(t,x)| = \left|\frac{x + S(t,\cdot)}{t}\right| = \left|\frac{\widetilde{S}(t,\cdot) + (I - C\bar{A}_t^{-1})x}{t}\right| \leq K_0 + K_2 t|x|,$$

which implies the velocity field $|V(t,x)|$ remains locally uniformly bounded and grows at most linearly.

Furthermore,

$$\|\nabla V(t,x)\|_\infty = \left\|\nabla\left(\frac{\widetilde{S}(t,x) + (I - C\bar{A}_t^{-1})x}{t}\right)\right\|_\infty \leq (K_1 + K_2)t,$$

which yields a Lipschitz constant that is uniform over space and independent of the dimension, ensuring uniform equicontinuity.

Next, we give the properties of $V(t,x)$ with respect to time over $(0,1)$. By taking equation 21, we have

$$\begin{aligned}
&\partial_t V(t,x)\\
=&\partial_t\left(\frac{\widetilde{S}(t,\cdot) + (I - C\bar{A}_t^{-1})x}{t}\right)\\
=&\partial_t\left(\frac{K(t)\sqrt{C}\int_{\mathbb{R}^d} G(t,x,y)\nabla_y h(\sqrt{C}y)\exp\left(h(\sqrt{C}y)\right)\mathrm{d}y}{t\int_{\mathbb{R}^d} G(t,x,y)\exp\left(h(\sqrt{C}y)\right)\mathrm{d}y}\right) + \partial_t\left(\frac{(I - C\bar{A}_t^{-1})x}{t}\right)\\
:=&A_1 + A_2
\end{aligned} \tag{22}$$

We begin by calculating the first part,

$$
\begin{aligned}
A_1 =& \partial_t \left(\frac{(A\bar{A}_t^{-1})\sqrt{C}\int_{\mathbb{R}^d} G(t,x,y)\nabla_y h(\sqrt{C}y)\exp\left(h(\sqrt{C}y)\right)\mathrm{d}y}{\int_{\mathbb{R}^d} G(t,x,y)\exp\left(h(\sqrt{C}y)\right)\mathrm{d}y} \right) \\
=& \frac{\partial_t(A\bar{A}_t^{-1})\sqrt{C}\int_{\mathbb{R}^d} G(t,x,y)\nabla_y h(\sqrt{C}y)\exp\left(h(\sqrt{C}y)\right)\mathrm{d}y}{\int_{\mathbb{R}^d} G(t,x,y)\exp\left(h(\sqrt{C}y)\right)\mathrm{d}y} \\
&+ \frac{A\bar{A}_t^{-1}\sqrt{C}\int_{\mathbb{R}^d} G(t,x,y)g(t,x,y)\exp\left(h(\sqrt{C}y)\right)\nabla_y h(\sqrt{C}y)dy}{\int_{\mathbb{R}^d} G(t,x,y)\exp\left(h(\sqrt{C}y)\right)\mathrm{d}y} \\
&- \frac{A\bar{A}_t^{-1}\sqrt{C}\int_{\mathbb{R}^d} G(t,x,y)\exp\left(h(\sqrt{C}y)\right)\nabla_y h(\sqrt{C}y)dy}{\int_{\mathbb{R}^d} G(t,x,y)\exp\left(h(\sqrt{C}y)\right)\mathrm{d}y} \\
&\cdot \frac{\int_{\mathbb{R}^d} G(t,x,y)g(t,x,y)\exp\left(h(\sqrt{C}y)\right)dy}{\int_{\mathbb{R}^d} G(t,x,y)\exp\left(h(\sqrt{C}y)\right)\mathrm{d}y} \\
\leq& \frac{\partial_t(A\bar{A}_t^{-1})\sqrt{C}\int_{\mathbb{R}^d} G(t,x,y)\nabla_y h(\sqrt{C}y)\exp\left(h(\sqrt{C}y)\right)\mathrm{d}y}{\int_{\mathbb{R}^d} G(t,x,y)\exp\left(h(\sqrt{C}y)\right)\mathrm{d}y} \\
&+ A\bar{A}_t^{-1}\sqrt{C}\,\mathrm{Cov}_{p_t(y|x)}\left(g(t,x,y), \nabla_y h(\sqrt{C}y)\right)
\end{aligned}
\tag{23}
$$

$$
\begin{aligned}
\leq& \frac{\partial_t(A\bar{A}_t^{-1})\sqrt{C}\int_{\mathbb{R}^d} G(t,x,y)\nabla_y h(\sqrt{C}y)\exp\left(h(\sqrt{C}y)\right)\mathrm{d}y}{\int_{\mathbb{R}^d} G(t,x,y)\exp\left(h(\sqrt{C}y)\right)\mathrm{d}y} \\
&+ A\bar{A}_t^{-1}\sqrt{C}\sqrt{\mathrm{Var}\left(g(t,x,y)\right)}\sqrt{\mathrm{Var}\left(\nabla_y h(\sqrt{C}y)\right)} \\
:=& I_1 + I_2,
\end{aligned}
$$

where

$$
p_t(y|x) = \frac{G(t,x,y)\exp\left(h(\sqrt{C}y)\right)}{\int_{\mathbb{R}^d} G(t,x,y)\exp\left(h(\sqrt{C}y)\right)\mathrm{d}y}.
$$

Define $K_3 := \sup_{0\leq t\leq 1} \|\frac{A\partial_t(\bar{A}_t^{-1})}{t}\| = \sup_{0\leq t\leq 1} \|2A(A-C)((At^2+C(1-t^2))^2)^{-1}\|$, we obtain the first term of A_1,

$$
\begin{aligned}
|I_1| &\leq \left\| 2A(A-C)\left(\left(At^2+C(1-t^2)\right)^2\right)^{-1} t \right\| |\sqrt{C}||\sqrt{C}\nabla h|_\infty \\
&\leq |\sqrt{C}||\sqrt{C}\nabla h|_\infty K_3 t \\
&\leq K_0 K_3 K^{-1}.
\end{aligned}
\tag{24}
$$

For the second term I_2 in equation 23, the analysis is carried out separately for the following two cases:

Case I - $\|B(t)\| \leq \frac{1}{2\|C\nabla^2 h\|_\infty}$: Then $p_t(y|x)$ is a log-concave measure as

$$-\nabla^2 \log p_t(y|x) = B(t)^{-1} - C\nabla^2 h \succ 0. \tag{25}$$

Then, by Brascamp-Lieb inequality, we have

$$\sqrt{\mathrm{Var}\left(g(t,x,y)\right)} \leq \sqrt{\mathbb{E}_{p_t(y|x)}\left|\nabla^T g(t,x,y)\Big(-\nabla^2 \log p_t(y|x)\Big)^{-1}\nabla g(t,x,y)\right|}, \tag{26}$$

here $g(t,x,y)$ is defined in equation 19 and its gradient is given by

$$\nabla g(t,x,y) = \partial_t K(t) B(t)^{-1}(\sqrt{C})^{-1}x - \partial_t B(t) B(t)^{-2}\left(K(t)(\sqrt{C})^{-1}x - y\right). \tag{27}$$

Recall that $K(t) = (A\bar{A}_t^{-1})t$, $B(t) = (A\bar{A}_t^{-1})(1-t^2)$.
Substituting equation 27 into equation 26 yields

$$\begin{aligned}
&\text{RHS of equation 26}\\
=&\Bigg(\int_{\mathbb{R}^d}\Big|\Big(\partial_t K(t)B(t)^{-1}(\sqrt{C})^{-1}x - \partial_t B(t)B(t)^{-2}\big(K(t)(\sqrt{C})^{-1}x - y\big)\Big)^T\\
&\quad\cdot\big(B(t)^{-1} - C\nabla^2 h\big)^{-1}\\
&\quad\cdot\Big(\partial_t K(t)B(t)^{-1}(\sqrt{C})^{-1}x - \partial_t B(t)B(t)^{-2}\big(K(t)(\sqrt{C})^{-1}x - y\big)\Big)\,p_t(y|x)\Big|\,\mathrm{d}y\Bigg)^{\frac{1}{2}}\\
\leq&\Bigg(\int_{\mathbb{R}^d}\Big|\big(\partial_t K(t)B(t)^{-1}C^{-1}x\big)^T\big(I - B(t)C\nabla^2 h\big)^{-1}\partial_t K(t)x\,p_t(y|x)\Big|\,\mathrm{d}y\\
&+\int_{\mathbb{R}^d}\Big|\big(-2\partial_t K(t)B(t)^{-1}(\sqrt{C})^{-1}\partial_t B(t)x\big)^T\big(I - B(t)C\nabla^2 h\big)^{-1}\\
&\quad\cdot\big(\big(K(t)(\sqrt{C})^{-1}x - y\big)B(t)^{-1}\big)\,p_t(y|x)\Big|\,\mathrm{d}y\\
&+\int_{\mathbb{R}^d}\Big|\big(K(t)(\sqrt{C})^{-1}x - y\big)^T B(t)^{-2}\big(\partial_t B(t)\big)^2\big(I - B(t)C\nabla^2 h\big)^{-1}\\
&\quad\cdot B(t)^{-1}\big(K(t)(\sqrt{C})^{-1}x - y\big)\,p_t(y|x)\Big|\,\mathrm{d}y\Bigg)^{\frac{1}{2}}.
\end{aligned}$$

Applying the triangle inequality $|a+b+c|^{\frac{1}{2}} \leq |a|^{\frac{1}{2}} + |b|^{\frac{1}{2}} + |c|^{\frac{1}{2}}$, we obtain:

$$\begin{aligned}
&\text{RHS of equation 26}\\
\leq&\left(\int_{\mathbb{R}^d}\Big|\left(\partial_t K(t)B(t)^{-1}C^{-1}x\right)^T\left(I - B(t)C\nabla^2 h\right)^{-1}\partial_t K(t)x\,p_t(y|x)\Big|\,\mathrm{d}y\right)^{\frac{1}{2}}\\
&+\Bigg(\int_{\mathbb{R}^d}\Big|-\Big(2\partial_t K(t)B(t)^{-1}(\sqrt{C})^{-1}\partial_t B(t)x\Big)^T\left(I - B(t)C\nabla^2 h\right)^{-1}\\
&\quad\cdot\Big(\big(K(t)(\sqrt{C})^{-1}x - y\big)B(t)^{-1}\Big)\,p_t(y|x)\Big|\,\mathrm{d}y\Bigg)^{\frac{1}{2}}
\end{aligned}$$

$$
\begin{aligned}
&+\left(\int_{\mathbb{R}^d}\Big|\left(K(t)(\sqrt{C})^{-1}x-y\right)^T B(t)^{-2}(\partial_t B(t))^2\right.\\
&\qquad\left.\cdot\left(I-B(t)C\nabla^2 h\right)^{-1}B(t)^{-1}\left(K(t)(\sqrt{C})^{-1}x-y\right)p_t(y|x)\Big|\,\mathrm{d}y\right)^{\frac{1}{2}}\\
:=&R_1+R_2+R_3.
\end{aligned}
$$

By a straightforward estimation,

$$
R_1\le|\partial_t K(t)|\|\sqrt{C}^{-1}\|\sqrt{\|B(t)\|^{-1}}\sqrt{(1-\|B(t)\|\|C\nabla^2 h\|)^{-1}}|x|.
$$

It follows from integration by parts that

$$
\begin{aligned}
&-\int_{\mathbb{R}^d}\left(K(t)(\sqrt{C})^{-1}x-y)B(t)^{-1}\right)p_t(y|x)\mathrm{d}y\\
=&-\frac{\int_{\mathbb{R}^d}\nabla_y G(t,x,y)\exp\left(h(\sqrt{C}y)\right)\mathrm{d}y}{\int_{\mathbb{R}^d}G(t,x,y)\exp\left(h(\sqrt{C}y)\right)\mathrm{d}y}\\
\le&|\sqrt{C}\nabla h|_\infty,
\end{aligned}
$$

which immediately implies

$$
\begin{aligned}
R_2=&\left(\frac{1}{\left|\int_{\mathbb{R}^d}G(t,x,y)\exp\left(h(\sqrt{C}y)\right)\mathrm{d}y\right|}\int_{\mathbb{R}^d}\Big|(-2\partial_t K(t)(\sqrt{C})^{-1}xB(t)^{-1}\partial_t B(t)\right.\\
&\qquad\left.\cdot\left(I-B(t)C\nabla^2 h\right)^{-1}\nabla_y G(t,x,y)\exp(h(\sqrt{C}y)\Big|\mathrm{d}y\right)^{\frac{1}{2}}\\
\le&\sqrt{2\|\partial_t K(t)\|\partial_t B(t)\|}|\nabla h|_\infty\sqrt{\|B(t)\|^{-1}}\sqrt{(1-\|B(t)\|\|C\nabla^2 h\|)^{-1}}\sqrt{|x|}.
\end{aligned}
$$

Similarly, applying integration by parts twice, we obtain

$$
\begin{aligned}
R_3\le&\|\partial_t B(t)\|\sqrt{\|C(|\nabla h|_\infty^2+\|\nabla^2 h\|_\infty)\|}\sqrt{\|B(t)^{-1}\|}\sqrt{(1-\|B(t)\|\|C\nabla^2 h\|_\infty)^{-1}}\\
&+\|\partial_t B(t)\|\|B(t)^{-1}\|\sqrt{(1-\|B(t)\|\|C\nabla^2 h\|_\infty)^{-1}}.
\end{aligned}
$$

Then we have

$$
\begin{aligned}
&\text{RHS of equation 26}\\
\le&\Big(|\partial_t K(t)x|^2\|C\|^{-1}+2\|\partial_t K(t)\|\|\partial_t B(t)\||\nabla h|_\infty|x|\\
&+\|\partial_t B(t)\|^2(\|C\nabla^2 h\|_\infty+|\sqrt{C}\nabla h|_\infty^2)\Big)^{\frac{1}{2}}\cdot\sqrt{\left(\|B(t)\|\left(1-\|B(t)\|\|C\nabla^2 h\|_\infty\right)\right)^{-1}}\\
&+\|\partial_t B(t)\|\sqrt{\left(\|B(t)\|^2(1-\|B(t)\|\|C\nabla^2 h\|_\infty)\right)^{-1}}.
\end{aligned}
$$

Combining with

$$
\sqrt{\mathrm{Var}\left(\nabla_y h(\sqrt{C}y)\right)}\le\|C\nabla^2 h\|_\infty\|\sqrt{B(t)}\|\sqrt{(1-\|B(t)\|\|C\nabla^2 h\|_\infty)^{-1}},
$$

we derive that

$$
\begin{aligned}
|I_2|\le&K\|C\nabla^2 h\|_\infty(1-\|B(t)\|\|C\nabla^2 h\|_\infty)^{-1}\Big(|\partial_t K(t)x|\\
&+\sqrt{2\|\partial_t K(t)\|\|\partial_t B(t)\||C\nabla h|_\infty|x|}+\|\partial_t B(t)\|\sqrt{\|C\nabla^2 h\|_\infty+|\sqrt{C}\nabla h|_\infty^2}\Big)\\
&+\|\sqrt{B(t)^{-1}}\|K\|\sqrt{C}\|\|\partial_t B(t)\|\|C\nabla^2 h\|_\infty(1-\|B(t)\|\|C\nabla^2 h\|_\infty)^{-1}
\end{aligned}
$$

$$
\begin{aligned}
&\leq 2K\|C\nabla^2 h\|_\infty \big(|\partial_t K(t)x| + \sqrt{2\|\partial_t K(t)\|\|\partial_t B(t)\||\nabla h|_\infty |x|} \\
&\quad + \|\partial_t B(t)\|\sqrt{\|C\nabla^2 h\|_\infty + |\sqrt{C}\nabla h|_\infty^2}\big) \\
&\quad + 2K\|\sqrt{C}\|\|\partial_t B(t)\|\|C\nabla^2 h\|_\infty \|\sqrt{B(t)^{-1}}\| \\
&\leq 2K_1 C_1|x| + 2\sqrt{2}K_1\sqrt{K_0}\sqrt{C_1}\sqrt{C_2}\sqrt{|x|} + 2K_1^{\frac{3}{2}}C_2 + 2K_1\|\sqrt{C}\|C_2\sqrt{\|B(t)\|^{-1}} \\
&\leq 3K_1 C_1|x| + \frac{2K^{-1}K_1\|\sqrt{C}\|C_2}{\sqrt{1-t^2}} + C_3,
\end{aligned}
$$

where the second inequality use the fact $(1-\|B(t)\|\|C\nabla^2 h\|_\infty)^{-1} \leq 2$ under Case I, while the last inequality is obtained using Young's inequality, C_1, C_2, C_3 are dimension-free constants defined in table 3.

Case II **-** $\|B(t)\| > \frac{1}{2\|C\nabla^2 h\|}$**:** According to the definition of variance

$$
\begin{aligned}
\mathrm{Var}(g(t,x,y)) &= \int_{\mathbb{R}^d} \big(g(t,x,y)\big)^2 p_t(y|x)\mathrm{d}y - \left(\int_{\mathbb{R}^d} g(t,x,y)p_t(y|x)\mathrm{d}y\right)^2 \\
&\leq \int_{\mathbb{R}^d} \big(g(t,x,y)\big)^2 p_t(y|x)\mathrm{d}y,
\end{aligned}
$$

We have the following estimate, analogous to the right-hand side of equation 26:

$$
\begin{aligned}
&\sqrt{\mathrm{Var}\left(g(t,x,y)\right)} \\
\leq &\frac{\|\sqrt{B(t)^{-1}}\|}{2}\Big(2\|\sqrt{C}^{-1}\||\partial_t K(t)x| + 2\sqrt{3}\sqrt{\|\partial_t K(t)\|\|\partial_t B(t)\||\nabla h|_\infty |x|} \\
&+ \sqrt{6}\|\partial_t B(t)\|\sqrt{\|C\nabla^2 h\|_\infty + |\sqrt{C}\nabla h|_\infty^2}\Big) \\
&+ |\partial_t K(t)x|\sqrt{\|\nabla^2 h\|_\infty + |\nabla h|_\infty^2} + \frac{1}{2}\|\partial_t B(t)\|\sqrt{|\sqrt{C}\nabla h|_\infty(\|C\nabla^2 h\|_\infty + |\sqrt{C}\nabla h|_\infty^2)} \\
&+ \sqrt{\|\partial_t K(t)\|\|\partial_t B(t)\||\nabla h|_\infty(\|C\nabla^2 h\|_\infty + |\sqrt{C}\nabla h|_\infty^2)|x|} + \frac{\sqrt{3}}{2}\|\partial_t B(t)\|\|B(t)^{-1}\| \\
\leq &\sqrt{\frac{\|\nabla^2 h\|_\infty}{2}}\Big(2|\partial_t K(t)x| + 2\sqrt{3}\sqrt{\|\partial_t K(t)\|\|\partial_t B(t)\||C\nabla h|_\infty |x|} \\
&+ \sqrt{6}\|\sqrt{C}\|\|\partial_t B(t)\|\sqrt{\|C\nabla^2 h\|_\infty + |\sqrt{C}\nabla h|_\infty^2}\Big) + |\partial_t K(t)x|\sqrt{\|\nabla^2 h\|_\infty + |\nabla h|_\infty^2} \\
&+ \sqrt{\|\partial_t K(t)\|\|\partial_t B(t)\||\nabla h|_\infty(\|C\nabla^2 h\|_\infty + |\sqrt{C}\nabla h|_\infty^2)|x|} \\
&+ \frac{1}{2}\|\partial_t B(t)\|\sqrt{|\sqrt{C}\nabla h|_\infty(\|C\nabla^2 h\|_\infty + |\sqrt{C}\nabla h|_\infty^2)} + \sqrt{3}\|\partial_t B(t)\|\|C\nabla^2 h\|_\infty.
\end{aligned}
$$

Together with

$$
\sqrt{\mathrm{Var}\left(\nabla_y h(\sqrt{C}y)\right)} \leq |\sqrt{C}\nabla h|_\infty,
$$

we obtain

$$
\begin{aligned}
|I_2| \leq & K|\sqrt{C}\nabla h|_\infty \Bigg(|\partial_t K(t)x| \big(\sqrt{2\|C\nabla^2 h\|_\infty} + \sqrt{(\|C\nabla^2 h\|_\infty + |\sqrt{C}\nabla h|_\infty^2)}\big) \\
& + \sqrt{6}\sqrt{\|C\nabla^2 h\|_\infty}\sqrt{\|\partial_t K(t)\|\|\partial_t B(t)\||C\nabla h|_\infty |x|} \\
& + \sqrt{\|\partial_t K(t)\|\|\partial_t B(t)\|\sqrt{C}\nabla h|_\infty (\|C\nabla^2 h\|_\infty + |\sqrt{C}\nabla h|_\infty^2)|x|} \\
& + \sqrt{3}\|\sqrt{C}\|\sqrt{\|C\nabla^2 h\|_\infty}\|\|\partial_t B(t)\|\|\sqrt{\|C\nabla^2 h\|_\infty + |\sqrt{C}\nabla h|_\infty^2} \\
& + \frac{1}{2}\|\sqrt{C}\|\|\partial_t B(t)\|\sqrt{|\sqrt{C}\nabla h|_\infty (\|C\nabla^2 h\|_\infty + |\sqrt{C}\nabla h|_\infty^2)} \\
& + \sqrt{3}\|\sqrt{C}\|\|\partial_t B(t)\|\|C\nabla^2 h\|_\infty \Bigg) \\
\leq & (1+\sqrt{2})K_0\sqrt{K_1}C_1|x| + (1+\sqrt{6})K_0^{\frac{3}{2}}\sqrt{K_1}\sqrt{C_1}\sqrt{C_2}|\sqrt{x}| \\
& + K_0 C_2 (2\sqrt{3}K_1 + \frac{1}{2}\sqrt{K_0}\sqrt{K_1}) \\
\leq & 2(1+\sqrt{2})K_0\sqrt{K_1}C_1|x| + C_4,
\end{aligned}
$$

where C_4 defined in table 3 is also constant indepent of dimension.

Combining the above two cases, we obtain

$$
|I_2| \leq \max\{3K_1C_1, 2(1+\sqrt{2})K_0\sqrt{K_1}C_1\}|x| + \frac{2K^{-1}K_1\|\sqrt{C}\|C_2}{\sqrt{1-t^2}} + \max\{C_3, C_4\}. \tag{28}
$$

Using equation 23, equation 24 and equation 28, we derive

$$
\begin{aligned}
|A_1| \leq & |I_1| + |I_2| \\
\leq & K_0K_3K^{-1} + \max\{3K_1C_1, 2(1+\sqrt{2})K_0\sqrt{K_1}C_1\}|x| \\
& + \frac{2K_1K^{-1}\|\sqrt{C}\|C_2}{\sqrt{1-t^2}} + \max\{C_3, C_4\}.
\end{aligned}
$$

The next step is to calculate the absolute value of the second term of equation 22, i.e.

$$
\begin{aligned}
|A_2| = & \left| \frac{-C\partial_t(\bar{A}_t^{-1})xt + (I - C\bar{A}_t^{-1})x}{t^2} \right| \\
\leq & \|2C(A-C)\big((At^2 + C(1-t^2))^2\big)^{-1}\||x| + K_2|x| \\
\leq & (K_4 + K_2)|x|.
\end{aligned}
$$

where $K_4 := \sup_{0\leq t\leq 1}\|\frac{C\partial_t(\bar{A}_t^{-1})}{t}\| = \sup_{0\leq t\leq 1}\|2C(A-C)\big((At^2 + C(1-t^2))^2\big)^{-1}\|$.

It then follows from equation 22 that

$$
|\partial_t V(t,x)| \leq |A_1| + |A_2| \leq K_5|x| + \frac{K_6}{\sqrt{1-t^2}} + K_7.
$$

where $K_5 = \max\{3K_1C_1, 2(1+\sqrt{2})K_0\sqrt{K_1}C_1\} + K_2 + K_4$, $K_6 = 2K_1K^{-1}\|\sqrt{C}\|C_2$, $K_7 = \max\{C_3, C_4\} + K_0K_3K^{-1}$.

When $t = 0$, by equation 14 in the subsequently stated well-posedness Lemma 11, we have

$$
|V(0,x)| = \left|\sqrt{C}\mathbb{E}_{\bar{p}_0}[X]\right| \lesssim K\|C\|^{1/2}\left|\sqrt{C}\nabla h\right|_\infty = K_0.
$$

Similarly, $\|\nabla V(0,\cdot)\|_\infty$ is also bounded by $K_1 + K_2$. Then we conclude that the velocity field $V(t,x)$ satisfied the condition of Theorem 9 for all $t \in [0,1]$.

For clarity, the coefficients are summarized in Table 3.

In corollary 19, we take $C = I_d$, $A = (1-(1-\delta)^2)I_d$, $\bar{A}_t = (1-t^2)I_d$. According to equation 17, we deduce the explicit for coefficients $K_0^*, K_1^*, K_2^*, K_3^*, K_4^*, K_5^*, K_6^*, K_7^*, K_9^*$ in Table 5. □

B.3 Proof of Lemma 11

Proof. First, we prove the velocity field $V(t,x)$ is well-defined at $t=0$ (equation 14 in Lemma 11), i.e.

$$V(0,x) := \lim_{t\to 0} V(t,x) = \lim_{t\to 0} \frac{x+S(t,x)}{t} = \sqrt{C}\mathbb{E}_{\bar{p}_0}[X].$$

Let $t \to 0$, then it yields

$$\lim_{t\to 0} V(t,x) = \lim_{t\to 0} \partial_t S(t,x) = \lim_{t\to 0}\left(\frac{C\nabla(\partial_t p_t(x))}{p_t(x)} - \frac{\partial_t p_t(x)}{p_t(x)} S(t,x)\right).$$

By simple calculation, it holds that

$$\begin{aligned}
&\frac{\nabla(\partial_t p_t(x))}{p_t(x)} \\
=& -\partial_t\left(\det B(t)\right)(2\det B(t))^{-1} d\left(-K(t)^T K(t)\big(CB(t)\big)^{-1} - \bar{A}_t^{-1}\right)(x^T x)x \\
&- \partial_t B(t)\big(2B(t)\big)^{-1} K(t)(\sqrt{C}B(t))^{-1}\int_{\mathbb{R}^d} y p(1,y|t,x)\mathrm{d}y \\
&+ \left(-K(t)\partial_t K(t)(CB(t))^{-1} - K(t)^T K(t)\partial_t\big(B(t)^{-1}\big)\big(2CB(t)\big)^{-1} - \frac{1}{2}\partial_t(\bar{A}_t^{-1})\right) \\
&\quad\cdot\Bigg(2x + \Big(-K(t)^T K(t)(CB(t))^{-1} - \bar{A}_t^{-1}\Big)(x^T x)x \\
&\qquad + 2K(t)\big(\sqrt{C}B(t)\big)^{-1}\int_{\mathbb{R}^d}(x^T y)x p(1,y|t,x)\mathrm{d}y\Bigg) \\
&+ \left(\partial_t K(t)\big(\sqrt{C}B(t)\big)^{-1} + K(t)\partial_t(B(t)^{-1})(\sqrt{C})^{-1}\right) \\
&\quad\cdot\Bigg(\int_{\mathbb{R}^d}\Big(y + K(t)(\sqrt{C}B(t))^{-1}(x^T y)y\Big)p(1,y|t,x)\mathrm{d}y \\
&\qquad + \int_{\mathbb{R}^d}\Big(-K(t)^T K(t)(CB(t))^{-1} - \bar{A}_t^{-1}\Big)(x^T y)x p(1,y|t,x)\mathrm{d}y\Bigg) \\
&- \frac{1}{2}\partial_t\big(B(t)^{-1}\big)\int_{\mathbb{R}^d}\left(\Big(-K(t)^T K(t)\big(CB(t)\big)^{-1} - \bar{A}_t^{-1}\Big)(y^T y)x\right)p(1,y|t,x)\mathrm{d}y \\
&- \frac{1}{2}\partial_t\big(B(t)^{-1}\big)\int_{\mathbb{R}^d} K(t)\big(\sqrt{C}B(t)\big)^{-1}(y^T y)y p(1,y|t,x)\mathrm{d}y,
\end{aligned}$$

while

$$\begin{aligned}
&\frac{\partial_t p_t(x)}{p_t(x)} \\
=& -\partial_t\left(\det B(t)\right)\big(2\det B(t)\big)^{-1} d \\
&+ x^T\left(-K(t)\partial_t K(t)\big(CB(t)\big)^{-1} - (2C)^{-1}K(t)K(t)^T\partial_t\big(B(t)^{-1}\big) - \frac{1}{2}\partial_t(\bar{A}_t^{-1})\right)x \\
&+ \int_{\mathbb{R}^d} x^T\left(\partial_t K(t)\big(\sqrt{C}B(t)\big)^{-1} + K(t)(\sqrt{C})^{-1}\partial_t\big(B(t)^{-1}\big)\right) y p(1,y|t,x)\,\mathrm{d}y \\
&- \int_{\mathbb{R}^d} y^T\frac{1}{2}\partial_t\big(B(t)^{-1}\big) y p(1,y|t,x)\,\mathrm{d}y.
\end{aligned}$$

From observing that

$$\lim_{t\to 0}\partial_t\left(\det B(t)\right)=0,\ \lim_{t\to 0}\partial_t B(t)=0,\ \lim_{t\to 0}K(t)=0,\ \lim_{t\to 0}\partial_t(\bar{A}_t^{-1})=0,$$

and Assumption 7, which ensures

$$\lim_{t\to 0}\int_{\mathbb{R}^d}|y|^3 p(1,y|t,x)\mathrm{d}y=\int_{\mathbb{R}^d}|y|^3\lim_{t\to 0}p(1,y|t,x)\mathrm{d}y=\mathbb{E}_{\bar{p}_0}[|X|^3]<+\infty,$$

we have

$$\lim_{t\to 0}\frac{\partial_t p_t(x)}{p_t(x)}S(t,x)=-\frac{x^\top x}{\sqrt{C}}\mathbb{E}_{\bar{p}_0}[X],\quad \lim_{t\to 0}\frac{C\nabla(\partial_t p_t(x))}{p_t(x)}=\sqrt{C}\mathbb{E}_{\bar{p}_0}[X]-\frac{x^\top x}{\sqrt{C}}\mathbb{E}_{\bar{p}_0}[X].$$

Therefore, it yields $\lim_{t\to 0}V(t,x)=\sqrt{C}\mathbb{E}_{\bar{p}_0}[X]$, which completes the proof of equation 14.

Next, together with the regularity of the velocity field (Theorem 9), the Arzelà-Ascoli theorem (Arzela, 1895) ensures the existence of a subsequence $\{V(t_k,\cdot)\}_{k\in N}$ with $t_k\to 0$ that converges locally uniformly to $V(0,\cdot)$, thereby guaranteeing the well-posedness of the ODE equation 7 on the entire time interval $t\in[0,1]$. □

B.4 Proof of Corollary 12

Proof. Recall the Föllmer flow equation 7 with $\|\nabla V(t,\cdot)\|_\infty\le(K_1+K_2)t$ in Theorem 9, by following the Theorem 1 in (Mikulincer & Shenfeld, 2023), we arrive at the following result,

$$\mathrm{Lip}(\overleftarrow{X}_1(x))\le\|\nabla\overleftarrow{X}_1(x)\|_{op}\le\exp\left(\int_0^1(K_1+K_2)s\mathrm{d}s\right)\le\exp\left(\frac{K_1+K_2}{2}\right).$$

□

B.5 Proof of Corollary 15

Proof. For any $x,y\in\mathbb{R}^d$, $t\in[t_n,t_{n+1}]$ with $k=0,1,\dots,N-1$, Itô's formula gives

$$\frac{\mathrm{d}|\overleftarrow{Y}_t(x)-\overleftarrow{Y}_t(y)|^2}{dt}=2\langle\overleftarrow{Y}_t(x)-\overleftarrow{Y}_t(y),\widetilde{V}\big(t_n,\overleftarrow{Y}_{t_n}(x)\big)-\widetilde{V}\big(t_n,\overleftarrow{Y}_{t_n}(y)\big)\rangle.$$

Using the Cauchy-Schwarz inequality, we obtain

$$\frac{\mathrm{d}|\overleftarrow{Y}_t(x)-\overleftarrow{Y}_t(y)|^2}{dt}\le 2\sqrt{|\overleftarrow{Y}_t(x)-\overleftarrow{Y}_t(y)|^2}\sqrt{|\widetilde{V}\big(t_n,\overleftarrow{Y}_{t_n}(x)\big)-\widetilde{V}\big(t_n,\overleftarrow{Y}_{t_n}(y)\big)|^2}.$$

Therefore,

$$\begin{aligned}\frac{d|\overleftarrow{Y}_t(x)-\overleftarrow{Y}_t(y)|}{dt}&\le|\widetilde{V}\big(t_n,\overleftarrow{Y}_{t_n}(x)\big)-\widetilde{V}\big(t_n,\overleftarrow{Y}_{t_n}(y)\big)|\\&\le\nabla\widetilde{V}|\overleftarrow{Y}_{t_n}(x)-\overleftarrow{Y}_{t_n}(y)|\\&\le(K_1+K_2+K_8)t_n|\overleftarrow{Y}_{t_n}(x)-\overleftarrow{Y}_{t_n}(y)|,\end{aligned}$$

where the last inequality uses Lipschitzness of $\widetilde{V}$ in Assumption 14. Integration over time yields

$$\begin{aligned}&|\overleftarrow{Y}_{t_{n+1}}(x)-\overleftarrow{Y}_{t_{n+1}}(y)|\\\le&|\overleftarrow{Y}_{t_n}(x)-\overleftarrow{Y}_{t_n}(y)|+(t_{n+1}-t_n)(K_1+K_2+K_8)t_n|\overleftarrow{Y}_{t_n}(x)-\overleftarrow{Y}_{t_n}(y)|.\end{aligned}$$

Then, it follows that the Lipschitz constant of the discrete flow satisfies $\mathrm{Lip}(\widetilde{T}_n)\le 1+(t_{n+1}-t_n)(K_1+K_2+K_8)t_n$. Iterating this bound over all $n=0,1,\dots,N-1$, we obtain the following estimate over the full

interval $[0,1]$,

$$|\overleftarrow{Y}_1(x) - \overleftarrow{Y}_1(y)| \leq \left(\prod_{n=0}^{N-1} \mathrm{Lip}(\widetilde{T}_n)\right) |\overleftarrow{Y}_{t_0}(x) - \overleftarrow{Y}_{t_0}(y)|$$
$$\leq \exp\left(\frac{K_1 + K_2 + K_8}{2}\right) |x - y|,$$

and conclude the proof. □

B.6 Proof of Theorem 16

Proof. Recall that Assumption 7, 8 ensure the well-podeness and Lipschitzness of Föllmer flow $(\overleftarrow{X}_t)_{t\in[0,1]}$ in equation 7, with

$$\mathrm{Lip}(T_n) \leq \exp\left(\int_{t_n}^{t_{n+1}} (K_1 + K_2)t dt\right) \quad \text{and} \quad \prod_{j=0}^{N-1} \mathrm{Lip}(T_j) \leq \exp\left(\frac{K_1 + K_2}{2}\right),$$

as established in Lemma 11 and Corollary 12.

Furthermore, Assumption 14 guarantees the Lipschitzness of learned discret Föllmer flow $(\overleftarrow{Y}_t)_{t\in[0,1]}$ in equation 10, with

$$\mathrm{Lip}(\widetilde{T}_n) \leq 1 + (t_{n+1} - t_n)(K_1 + K_2 + K_8)t_n \text{ and } \prod_{j=0}^{N-1} \mathrm{Lip}(\widetilde{T}_j) \leq \exp\left(\frac{K_1 + K_2 + K_8}{2}\right),$$

as shown in Corollary 15.

Therefore, it only remains to verify that the stepwise approximation error *satisfies Assumption 5.* To analyze the discretization error at each step, we recall the expression in equation 2:

$$T_n(\overleftarrow{X}_{t_n}) = \overleftarrow{X}_{t_{n+1}}.$$

Applying the vector-valued Taylor expansion of $\overleftarrow{X}_{t_{n+1}}$ over $[t_n, t_{n+1}]$, the remainder is defined by

$$R(t) := T_n(\overleftarrow{X}_{t_n}) - \overleftarrow{X}_{t_n} - hV(t_n, \overleftarrow{X}_{t_n}).$$

Under Assumption 7, we can derive the second moment bound by the forward diffusion process equation 5

$$\mathbb{E}_{\bar{p}_t}|\overrightarrow{X}_t|^2 = \mathbb{E}_{\bar{p}_t}|\overrightarrow{X}_t - (1-t)\overrightarrow{X}_0|^2 + \mathbb{E}_{\bar{p}_t}|(1-t)\overrightarrow{X}_0|^2$$
$$\leq t(2-t)Tr(C) + (1-t)^2 M_2 \leq M_0.$$

Then the expectation of the $R(t)$ is controlled by

$$\mathbb{E}|R(t)|^2 = \mathbb{E}_{\overleftarrow{X}_{t_n}\sim\overleftarrow{P}_{t_n}} |T_n(\overleftarrow{X}_{t_n}) - \overleftarrow{X}_{t_n} - hV(t_n, \overleftarrow{X}_{t_n})|^2$$
$$\leq \frac{h^4}{4} \sup_{\tau\in(t_n,t_{n+1})} \mathbb{E}_{\overleftarrow{X}_\tau\sim\overleftarrow{P}_\tau} |\partial_\tau V(\tau, \overleftarrow{X}_\tau)|^2$$
$$\leq \frac{3h^4}{4}\left(K_5^2 M_0 + \frac{K_6^2}{1-t^2} + K_7^2\right), \quad \forall t \in [0,1),$$

where the last inequality follows from the bound on $|\partial_t V(t,x)|$ in Theorem 9, which gives

$$\mathbb{E}_{\overleftarrow{X}_\tau\sim\overleftarrow{P}_\tau} |\partial_\tau V(\tau, \overleftarrow{X}_\tau))|^2 \leq 3\left(K_5^2 M_0 + \frac{K_6^2}{1-\tau^2} + K_7^2\right).$$

Consequently, the local truncation error is bounded by

$$
\begin{aligned}
&\sqrt{\mathbb{E}_{\overleftarrow{X}_{t_n}\sim\overleftarrow{P}_{t_n}}|T_n(\overleftarrow{X}_{t_n})-\widetilde{T}_n(\overleftarrow{X}_{t_n})|^2}\\
=&\sqrt{\mathbb{E}_{\overleftarrow{X}_{t_n}\sim\overleftarrow{P}_{t_n}}|\overleftarrow{X}_{t_n}+hV(t_n,\overleftarrow{X}_{t_n})+R(t_n)-\overleftarrow{X}_{t_n}-h\widetilde{V}(t_n,\overleftarrow{X}_{t_n})|^2}\\
\leq&\sqrt{h^2\mathbb{E}_{\overleftarrow{X}_{t_n}\sim\overleftarrow{P}_{t_n}}|V(t_n,\overleftarrow{X}_{t_n})-\widetilde{V}(t_n,\overleftarrow{X}_{t_n})|^2}+\sqrt{\mathbb{E}|R(t_n)|^2}\\
\leq& h\left(\frac{\sqrt{3}}{2}\Big(K_5\sqrt{M_0}+\frac{K_6}{\sqrt{1-t_n^2}}h+K_7\Big)h+\epsilon\right).
\end{aligned}
\tag{29}
$$

The second inequality holds by the error between $\widetilde{V}(t_n,x)$ and $V(t_n,x)$ stated in Assumption 13. This completes the verification of Assumption 5.

Now in Theorem 6, we employ coupling between $\overleftarrow{X}_0\sim\overrightarrow{P}_1=\gamma_C$ and $\overleftarrow{Y}_0\sim\overleftarrow{Q}_0=\gamma_C$,

$$
\begin{aligned}
\mathcal{W}_2(\overleftarrow{P}_1,\overleftarrow{Q}_1)\leq&\exp\left(\frac{K_1+K_2+K_8}{2}\right)\mathcal{W}_2(\overleftarrow{P}_0,\overleftarrow{Q}_0)\\
&+\frac{\exp\left(\frac{K_1+K_2+K_8}{2}\right)-1}{((K_1+K_2+K_8)h)/2}\cdot h\left(\frac{\sqrt{3}}{2}\left(K_5\sqrt{M_0}+K_7\right)h+\epsilon\right)\\
&+\exp\left(\frac{K_1+K_2+K_8}{2}\right)\frac{\sqrt{3}K_6\pi}{4}h\\
\leq&\exp\left(\frac{K_1+K_2+K_8}{2}\right)\left(\sqrt{3}\left(K_5\sqrt{M_0}+K_9\right)h+2\epsilon\right).
\end{aligned}
\tag{30}
$$

where a straightforward calculation shows $\sum_{n=0}^{N-1}\frac{K_6}{\sqrt{1-t_n^2}}=\frac{K_6\pi}{2}$; Accordingly, set $K_9:=\frac{K_6\pi}{4}+K_7$. Noting that $\overleftarrow{P}_1=\overrightarrow{P}_0$, we obtain the conclusion in equation 16. □

Note that the first term in Theorem 6, stemming from the time-propagating discrepancy of the semigroup maps, vanishes in Theorem 16 because the Föllmer flow $(\overleftarrow{X}_t)_{t\in[0,1]}$ is well-posed at $t=0$, giving $\mathcal{W}_2(\overleftarrow{P}_0,\overleftarrow{Q}_0)=0$. Thus, only the accumulated discretization error remains, corresponding to the second term in Theorem 6.

B.7 Result under the relaxation of Assumption 14

Remark 23 (Relaxation of Assumption 14)**.** *Assumption 3.13 can be relaxed as follows. We only require that for all $k\in\{0,1,\dots,N-1\}$,*

$$
\sum_{n=0}^{N-1}(t_{n+1}-t_n)\|\nabla\widetilde{V}(t_n,\cdot)\|_\infty\leq B,
\tag{31}
$$

for some constant $B>0$. Under this condition, the Lipschitz bound stated in Corollary 15 is refined to $\exp(B)$*. Consequently, Theorem 16 remains valid with the product of Lipschitz coefficient $\prod_{j=0}^{N-1}\mathrm{Lip}(\widetilde{T}_j)$, where the factor* $\exp\left(\frac{K_1+K_2+K_8}{2}\right)$ *is replaced throughout by* $\exp(B)$*.*

Proof. Denote $\beta_n=\|\nabla\widetilde{V}(t_n,\cdot)\|_\infty$, then

$$
\frac{d|\overleftarrow{Y}_t(x)-\overleftarrow{Y}_t(y)|}{dt}\leq|\widetilde{V}\big(t_n,\overleftarrow{Y}_{t_n}(x)\big)-\widetilde{V}\big(t_n,\overleftarrow{Y}_{t_n}(y)\big)|\leq\beta_n|\overleftarrow{Y}_{t_n}(x)-\overleftarrow{Y}_{t_n}(y)|.
$$

Integration over time yields

$$|\overleftarrow{Y}_{t_{n+1}}(x) - \overleftarrow{Y}_{t_{n+1}}(y)| \leq |\overleftarrow{Y}_{t_n}(x) - \overleftarrow{Y}_{t_n}(y)| + (t_{n+1} - t_n)\beta_n |\overleftarrow{Y}_{t_n}(x) - \overleftarrow{Y}_{t_n}(y)|,$$

yielding $\mathrm{Lip}(\widetilde{T}_n) \leq 1 + (t_{n+1} - t_n)\beta_n$. Recall equation 31, we obtain

$$\mathrm{Lip}(\overleftarrow{Y}_1(x)) \leq \prod_{j=0}^{N-1} \mathrm{Lip}(\widetilde{T}_j) \leq \exp\left(\sum_{n=0}^{N-1} (t_{n+1} - t_n)\beta_n\right) = \exp(B). \tag{32}$$

Subsequently, we analyze the impact of relaxing Assumption 14 on convergence. The preliminary estimate equation 29 still hold. Under the new Lipschitz coefficient $\mathrm{Lip}(\widetilde{T}_n) \leq 1 + (t_{n+1} - t_n)\beta_n$, equation equation 30 takes the following form,

$$\begin{aligned}
\mathcal{W}_2(\overleftarrow{P}_1, \overleftarrow{Q}_1) \leq & \exp(B)\, \mathcal{W}_2(\overleftarrow{P}_0, \overleftarrow{Q}_0) + \exp(B)\, \frac{\sqrt{3} K_6 \pi}{4} h \\
& + \frac{\exp(B)}{h} \cdot h \left(\frac{\sqrt{3}}{2} \left(K_5 \sqrt{M_0} + K_7 \right) h + \epsilon \right) \\
\leq & \exp(B) \left(\frac{\sqrt{3}}{2} \left(K_5 \sqrt{M_0} + K_9 \right) h + \epsilon \right).
\end{aligned} \tag{33}$$

where K_5 and K_9 are same with Theorem 16. □

B.8 Relation to Prob ODE

The probabilistic ODE (Prob ODE) (Song et al., 2021; Gao & Zhu, 2025)

$$\frac{d\widehat{X}_s}{ds} = -(\widehat{X}_s - \nabla \log \widehat{p}_s(\widehat{X}_s)), \quad s \in [T, 0], \tag{34}$$

can be viewed as a time-rescaled Föllmer flow, via $s \mapsto \ln\left(\frac{1}{t}\right)$, where T is finite time. Since Lipschitzness of the transport maps are invariant under time rescaling, the results of Corollary 17 apply directly to the equation 34. The discretization can be chosen as

$$s_n = \ln\left(\frac{1}{t_n}\right), \quad n = 1, \ldots, N.$$

In the forward Prob ODE, the distribution approaches Gaussian only as $s \to +\infty$. To realize this limit in practice, we set $s_0 = +\infty$ and initialize the dynamics with $\widehat{X}_{s_0} \sim \mathcal{N}(0, C)$, and take $T = s_1 = \ln\left(\frac{1}{t_1}\right)$ with $\widehat{X}_{s_1} = \widehat{X}_{s_0} + t_1\sqrt{C}\mathbb{E}_{\bar{p}_0}[X]$, which corresponds to a single-step first-order Euler method. For n-step ($n \geq 2$), the update $\widehat{X}_{s_n} = \widehat{X}_{s_{n-1}} + (e^{s_{n-1} - s_n} - 1)\Big(S_\theta(e^{-s_{n-1}}, \widehat{X}_{s_{n-1}}) + \widehat{X}_{s_{n-1}}\Big)$ follows the exponential Euler scheme.

B.9 Proof of convergence theory of 1-rectified flow

Proof. The forward process in the first-step rectification (Liu et al., 2023; Rout et al., 2024), constructed by independently coupling the data with a standard Gaussian reference distribution, is defined by the interpolation $\hat{X}_t = \hat{\alpha}_t \hat{X}_1 + \hat{\beta}_t \mathcal{N}$ with $\hat{\alpha}_t = 1 - t, \hat{\beta}_t = t$. Then the transition probability distribution from $\hat{X}_0$ to $\hat{X}_t$ is given by

$$\hat{X}_t | \hat{X}_1 = x_1 \sim \mathcal{N}\big((1-t)x_1, tI_d\big). \tag{35}$$

Under the Gaussian tail Assumption 8, the score function can be calculated by

$$\hat{S}(t, x) := \nabla \log \hat{p}_t = \nabla \log \int_{\mathbb{R}^d} \Big(2\pi \det(\hat{B}(t))\Big)^{-\frac{d}{2}} G(t, x, y) \cdot \exp\left(-\frac{|x|_{\hat{A}_t}}{2}\right) \exp(h(y))\, \mathrm{d}y,$$

where $G(t,x,y) := \exp\left(-\frac{|\hat{K}(t)x-y|^2_{\hat{B}(t)}}{2}\right)$, $\hat{A}_t = At^2 + (1-t)^2 I_d$, $\hat{K}(t) = (A\hat{A}_t^{-1})t$, $\hat{B}(t) = (A\hat{A}_t^{-1})(1-t)^2$. First, we consider the modified score function:

$$\widetilde{\hat{S}}(t,x) := \hat{S}(t,x) + \hat{A}_t^{-1}x \leq |\hat{K}(t)\nabla h(x)|.$$

Let $\hat{K} = \sup_{0\leq t\leq 1} |\frac{1}{t}\hat{K}(t)| = \sup_{0\leq t\leq 1} |A\hat{A}_t^{-1}| \leq 1 + \|A\|$, then we have

$$|\widetilde{\hat{S}}(t,\cdot)|_\infty \leq \hat{K}|\nabla h|_\infty t = \hat{K}_0 t$$

with $\hat{K}_0 := \hat{K}|\nabla h|_\infty$.
Taking the derivative twice along that direction and using the same method as above, it yields

$$\|\nabla\widetilde{\hat{S}}(t,\cdot)\|_\infty \leq \hat{K}(t)^2(\|\nabla^2 h\|_\infty + |\nabla h|^2_\infty) = \hat{K}_1 t^2,$$

where $\hat{K}_1 := \hat{K}^2(\|\nabla^2 h\|_\infty + |\nabla h|^2_\infty)$. Define $\hat{K}_2 := \sup_{0\leq t\leq 1} \|\frac{1}{t}\big(I_d - (1-t)\hat{A}_t^{-1}\big)\| = \sup_{0\leq t\leq 1} \|(A + C - I_d)\big(At^2 + (1-t)^2 I_d\big)^{-1}\|$, we obtain

$$|\hat{V}(t,x)| := \left|\frac{x + (1-t)\hat{S}(t,\cdot)}{t}\right| = \left|\frac{(1-t)\widetilde{\hat{S}}(t,\cdot) + \big(I_d - (1-t)\hat{A}_t^{-1}\big)x}{t}\right| \leq \hat{K}_0 + \hat{K}_2|x|,$$

and

$$\|\nabla\hat{V}(t,x)\|_\infty = \left\|\nabla\left(\frac{(1-t)\widetilde{\hat{S}}(t,\cdot) + (I_d - (1-t)\hat{A}_t^{-1})x}{t}\right)\right\|_\infty \leq \hat{K}_1 t + \hat{K}_2.$$

Similar to the proof of $|\partial_t V|$ of Föllmer flow in Appendix B.2, we derive

$$|\partial_t\hat{V}(t,x)| \leq \hat{K}_5|x| + \frac{\hat{K}_6}{\sqrt{1-t^2}} + \hat{K}_7.$$

where $\hat{K}_5, \hat{K}_6$ and $\hat{K}_7$ are dimension-free constants. This completes the argument that the trajectory $\hat{X}_t$ of 1-rectified flow possesses the similar regularity properties for its velocity field as those established in Theorem 9. Consequently, by following the proof steps of Theorem 16 in Appendix B.6, the desired result directly follows. □

B.10 Convergence in the Bayesian Inverse problems

We are aware of several posterior analyses, such as Bayesian inverse problems (van de Schoot et al., 2021), used in uncertainty quantification to infer model parameters x from observations $y \in \mathbb{R}^m$. The posterior typically takes the form of

$$\bar{p}_0(x) = D_0 \exp\left(-\frac{|x|^2_C}{2}\right)\exp\left(-\frac{|G(x)-y|^2_\Sigma}{2}\right), \tag{36}$$

where D_0 is a normalizing constant, C denotes the covariance matrix of the Gaussian prior, Σ represents the covariance of the observational noise and $G \in C^b_2(\mathbb{R}^d, \mathbb{R}^m)$ is a nonlinear forward operator. In our training framework, we adopt the Gaussian prior with covariance C from equation 36 as the invariant measure of the forward diffusion process equation 5. The conditioned score (Batzolis et al., 2021) in the score matching is trained by minimizing

$$\mathbb{E}_{\bar{p}_t(x;y)}\big|\widetilde{s}(1-t,x;y) - C\nabla_x \log\bar{p}_t(x;y)\big|^2,$$

where $\bar{p}_t$ denotes the joint law of (X_t, Y) with $Y = G(X_0) + \mathcal{N}(0,\Sigma)$. For ODE-based generation of the posterior distribution with observation y, we impose the following assumption on the approximation error of the velocity field $V(t,x;y)$ given in equation 7.

Assumption 24. *Fixing observation y, for each time discretization point t_n,*

$$\mathbb{E}_{\overrightarrow{P}_{1-t_n};y}|V(t_n,x;y)-\widetilde{V}(t_n,x;y)|^2 \le \epsilon^2.$$

Theorem 25. *Suppose third moment Assumption 7, accuracy Assumption 24 and regularity Assumption 14 hold. Using the Euler method to the Föllmer flow with uniform step size $h = t_{n+1} - t_n \le 1$ yields,*

$$\mathcal{W}_2(\overrightarrow{P}_0(\cdot,y),\overleftarrow{Q}_1(\cdot,y)) \le \exp\left(\frac{\widetilde{K_1}+K_8}{2}\right)\left(\frac{\sqrt{3}}{N}\left(\widetilde{K_5}\sqrt{M_0}+\widetilde{K_9}\right)+2\epsilon\right). \tag{37}$$

where $\widetilde{K_1}, \widetilde{K_5}, \widetilde{K_9}$ are dimension-free constants depending on $(\|C\|, \|\Sigma\|, \|G\|_{C_2}, |y|)$, see Table 4 of Appendix C , and the constant K_8 is defined in Assumption 14.

Proof. Take $A = C$, and $h(x) = -\frac{|G(x)-y|_\Sigma^2}{2}$, then $h(x)$ satisfies,

$$\begin{aligned}
|\sqrt{C}\nabla h(x)| &= |\sqrt{C}\nabla G(x)\Sigma^{-1}(G(x)-y)| \le \|C\|^{\frac{1}{2}}\left(|G|_\infty + |y|\right)\|\Sigma^{-1}\|\|\nabla G\|_\infty,\\
\|C\nabla^2 h(x)\| &= \|C\nabla^2 G(x)\Sigma^{-1}(G(x)-y) + C\nabla G(x)\Sigma^{-1}\nabla G(x)^T\|\\
&\le \|C\|\|\Sigma\|^{-1}\|\nabla^2 G\|_\infty(|G|_\infty + |y|\|\nabla G\|_\infty^2).
\end{aligned}$$

Then by Theorem 16, we obtain the bound equation 37 with the constants replaced as specified in Table 4. □

Remark 26. *With fixed $\widetilde{K}_1$, $\widetilde{K}_5$ and $\widetilde{K}_9$, for ϵ_0 accuracy in W_2 distance for 37, one requires at most:*

$$N = \mathcal{O}\left(\frac{\sqrt{M_0}}{\epsilon_0}\right), \quad \epsilon = \mathcal{O}(\epsilon_0).$$

C Tables of Constants

In this part, we provide the detailed proofs of the theories in Theorem 9, Theorem 16, Theorem 25, Corollary 19 and Theorem 20.

Table 3: Explicit for coefficients in Thm. 9 and Thm. 16.

Coefficient	**Explicit expressions**
$\bar{A}_t$	$At^2 + C(1-t^2)$
$K(t)$	$(A\bar{A}_t^{-1})t$
$B(t)$	$(A\bar{A}_t^{-1})(1-t^2)$
K	$\sup_{0\le t\le 1}\lvert A\bar{A}_t^{-1}\rvert \le \max\{1, \|AC^{-1}\|\}$
K_0	$K\|C\|^{1/2}\lvert\sqrt{C}\nabla h\rvert_\infty$
K_1	$K^2(\|C\nabla^2 h\|_\infty + \lvert\sqrt{C}\nabla h\rvert_\infty^2)$
K_2	$\sup_{0\le t\le 1}\|\frac{1}{t^2}(I - C\bar{A}_t^{-1})\| = \sup_{0\le t\le 1}\|(A-C)(At^2+C(1-t^2))^{-1}\|$
K_3	$\sup_{0\le t\le 1}\|\frac{A\partial_t(\bar{A}_t^{-1})}{t}\| = \sup_{0\le t\le 1}\|2A(A-C)\big((At^2+C(1-t^2))^2\big)^{-1}\|$
K_4	$\sup_{0\le t\le 1}\|\frac{C\partial_t(\bar{A}_t^{-1})}{t}\| = \sup_{0\le t\le 1}\|2C(A-C)\big((At^2+C(1-t^2))^2\big)^{-1}\|$
K_5	$\max\{3K_1C_1, 2(1+\sqrt{2})K_0\sqrt{K_1}C_1\} + K_2 + K_4$
K_6	$2K_1K^{-1}\|C\|^{\frac{1}{2}}C_2$
K_7	$\max\{C_3, C_4\} + K_0K_3K^{-1}$
K_9	$\frac{1}{4}K_6\pi + K_7$
C_1	$\max_{t\in[\sqrt{1-\frac{1}{2\|C\|\|\nabla^2 h\|_\infty}},1)}\{\partial_t K(t)\} = \max\{\frac{\|A\|(\|(A-C)(1-\frac{1}{2\|C\|\|\nabla^2 h\|_\infty})-C\|)}{(\|C\|+\|(A-C)\|(1-\frac{1}{2\|C\|\|\nabla^2 h\|_\infty}))^2}, \frac{\|A-2C\|}{\|A\|}, \frac{\|A\|}{8\|C\|}\}$
C_2	$\max_{t\in[\sqrt{1-\frac{1}{2\|C\|\|\nabla^2 h\|_\infty}},1)}\{\partial_t B(t)\} = \max\{2, \frac{2\|A\|^2\sqrt{1-\frac{1}{2\|C\|\|\nabla^2 h\|_\infty}}}{(\|C\|+\|(A-C)\|(1-\frac{1}{2\|C\|\|\nabla^2 h\|_\infty}))^2}, \frac{9A^2}{8\|C\|^2}\sqrt{\frac{\|C\|}{3\|A-C\|}}\}$
C_3	$2K_1C_2(K_1^{\frac{1}{2}} + K_0)$
C_4	$2\sqrt{3}K_0K_1C_2 + \frac{1}{2}K_0^{\frac{3}{2}}K_1^{\frac{1}{2}}C_2 + \frac{(1+\sqrt{6})^2}{4(1+\sqrt{2})}K_0^2K_1^{\frac{1}{2}}C_2$

Table 4: Explicit for coefficients in Thm. 25.

Coefficient	**Explicit expressions**
$\widetilde{K_0}$	$\|C\|\|\Sigma^{-1}\|\,\|\nabla G\|_\infty\,(\|G\|_\infty + \|y\|)$
$\widetilde{K_1}$	$\|C\|\Big(\|\Sigma^{-1}\|\big(\|\nabla G\|_\infty^2 + (\|G\|_\infty + \|y\|)\|\nabla^2 G\|_\infty\big) + \|\Sigma^{-2}\|\,\|\nabla G\|_\infty^2\,(\|G\|_\infty + \|y\|)^2\Big)$
$\widetilde{K_5}$	$\max\{3\widetilde{K_1}, 2(1+\sqrt{2})\widetilde{K_0}\widetilde{K_1}^{\frac{1}{2}}\}$
$\widetilde{K_6}$	$4\|C\|^{\frac{1}{2}}\widetilde{K_1}$
$\widetilde{K_7}$	$\max\{\widetilde{C_3}, \widetilde{C_4}\}$
$\widetilde{K_9}$	$\|C\|^{\frac{1}{2}}\widetilde{K_1}\pi + \widetilde{K_7}$
$\widetilde{C_3}$	$4\widetilde{K_1}(\widetilde{K_1}^{\frac{1}{2}} + \widetilde{K_0})$
$\widetilde{C_4}$	$4\sqrt{3}\widetilde{K_0}\widetilde{K_1} + \widetilde{K_0}^{\frac{3}{2}}\widetilde{K_1}^{\frac{1}{2}} + \frac{(1+\sqrt{6})^2}{2(1+\sqrt{2})}\widetilde{K_0}^2\widetilde{K_1}^{\frac{1}{2}}$

Table 5: Explicit for coefficients in Cor. 19 and Thm. 20.

Coefficient	**Explicit expressions**
$\bar{A}_t$	$(1-t^2)I_d$
K_0^*	$\frac{R}{1-(1-\delta)^2}$
K_1^*	$3\left(\frac{R}{1-(1-\delta)^2}\right)^2$
K_2^*	$\sup_{t\le 1-\delta}\|\frac{1}{t^2}(I-\bar{A}_t^{-1})\| = \frac{1}{1-(1-\delta)^2}$
K_3^*	$\frac{2}{1-(1-\delta)^2}$
K_4^*	$\frac{2}{(1-(1-\delta)^2)^2}$
K_5^*	$\frac{9C_1^*R^2}{(1-(1-\delta)^2)^2} + \frac{2}{(1-(1-\delta)^2)^2} + \frac{1}{1-(1-\delta)^2}$
K_6^*	$\frac{6C_2^*R^2}{(1-(1-\delta)^2)^2}$
K_7^*	$6(\sqrt{3}+1)\left(\frac{R}{1-(1-\delta)^2}\right)^3 C_2^* + \frac{2R}{(1-(1-\delta)^2)^2}$
K_9^*	$\frac{3\pi}{2}\,\frac{C_2^*R^2}{(1-(1-\delta)^2)^2} + 6(\sqrt{3}+1)\,\frac{C_2^*R^3}{(1-(1-\delta)^2)^3} + \frac{2R}{(1-(1-\delta)^2)^2}.$
C_1^*	$\max\{\frac{(1-(1-\delta)^2)\|(1-\delta)^2(1-\frac{1}{2\|\nabla^2 h\|_\infty})-1\|}{\|1+(1-\delta)^2(1-\frac{1}{2\|\nabla^2 h\|_\infty})\|^2}, \frac{\|-(1-\delta)^2-1\|}{\|1-(1-\delta)^2\|}, \frac{\|1-(1-\delta)^2\|}{8}\},$
C_2^*	$\max\{2, \frac{2(1-(1-\delta)^2)^2(1-\frac{1}{2\|\nabla^2 h\|_\infty})^{\frac{1}{2}}}{\|1+(1-\delta)^2(1-\frac{1}{2\|\nabla^2 h\|_\infty})\|^2}, \frac{9(1-(1-\delta)^2)^2}{8\sqrt{3}(1-\delta)},$